Biogeosciences, 15, 4333–4352, 2018
https://doi.org/10.5194/bg-15-4333-2018
© Author(s) 2018. This work is distributed under
the Creative Commons Attribution 4.0 License.

Biogeosciences Open Access EGU

Modelling N_2 fixation related to *Trichodesmium* sp.: driving processes and impacts on primary production in the tropical Pacific Ocean

Cyril Dutheil[1,2], Olivier Aumont[2], Thomas Gorguès[3], Anne Lorrain[4], Sophie Bonnet[5], Martine Rodier[6], Cécile Dupouy[1,5], Takuhei Shiozaki[7], and Christophe Menkes[1,2]

[1]Centre IRD, Nouméa, New Caledonia
[2]LOCEAN Laboratory, IPSL, Sorbonne Universités (UPMC, Univ Paris 06)-CNRS-IRD-MNHN, Paris, France
[3]Laboratoire d'Océanographie Physique et Spatiale (LOPS), Univ. Brest-CNRS-Ifremer-IRD, Plouzané, France
[4]LEMAR, UMR 6539, UBO-CNRS-Ifremer-IRD, IUEM, Plouzané, France
[5]Aix Marseille Université, CNRS/INSU, Université de Toulon, IRD, Mediterranean Institute of Oceanography (MIO) UM 110, 13288, Marseille, France
[6]Environnement Insulaire Océanien (EIO), UMR 241 (Univ. de Polynésie Française, IRD, ILM, IFREMER), Tahiti, French Polynesia
[7]Research and Development Center for Global Change, Japan Agency for Marine-Earth Science and Technology, Yokosuka, Japan

Correspondence: Cyril Dutheil (cyril.dutheil@ird.fr)

Received: 24 December 2017 – Discussion started: 15 January 2018
Revised: 29 May 2018 – Accepted: 3 July 2018 – Published: 18 July 2018

Abstract. Dinitrogen fixation is now recognized as one of the major sources of bio-available nitrogen in the ocean. Thus, N_2 fixation sustains a significant part of the global primary production by supplying the most common limiting nutrient for phytoplankton growth. The "Oligotrophy to UlTra-oligotrophy PACific Experiment" (OUTPACE) improved the data coverage of the western tropical South Pacific, an area recently recognized as a hotspot of N_2 fixation. This new development leads us to develop and test an explicit N_2 fixation formulation based on the *Trichodesmium* physiology (the most studied nitrogen fixer) within a 3-D coupled dynamical–biogeochemical model (ROMS-PISCES). We performed a climatological numerical simulation that is able to reproduce the main physical (e.g. sea surface temperature) and biogeochemical patterns (nutrient and chlorophyll concentrations, as well as N_2 fixation) in the tropical Pacific. This simulation displayed a *Trichodesmium* regional distribution that extends from 150° E to 120° W in the south tropical Pacific, and from 120° E to 140° W in the north tropical Pacific. The local simulated maximuma were found around islands (Hawaii, Fiji, Samoa, New Caledonia, Vanuatu). We assessed that 15 % of the total primary production may be due to *Trichodesmium* in the low-nutrient low-chlorophyll regions (LNLC) of the tropical Pacific. Comparison between our explicit and the often used (in biogeochemical models) implicit parameterization of N_2 fixation showed that the latter leads to an underestimation of N_2 fixation rates by about 25 % in LNLC regions. Finally, we established that iron fluxes from island sediments control the spatial distribution of *Trichodesmium* biomasses in the western tropical South Pacific. Note, this last result does not take into account the iron supply from rivers and hydrothermal sources, which may well be of importance in a region known for its strong precipitation rates and volcanic activity.

1 Introduction

Nitrogen is known to be the most common limiting nutrient for phytoplankton growth in the modern world ocean (Moore et al., 2013), especially in the low-nutrient low-chlorophyll (LNLC) ecosystems (Arrigo, 2005; Gruber, 2005). Characterizing the processes governing nitrogen sources and sinks

to and from the ocean is therefore central to understanding oceanic production, organic matter export, and food-web structure. Atmospheric dinitrogen (N_2) dissolved in seawater is by far the dominant form of N present in the ocean, i.e. the $N_2 : NO_3^-$ ratio typically exceeds 100 in surface waters. However, most phytoplankton species cannot assimilate N_2, and only grow using reactive forms of nitrogen such as nitrate, ammonium, and dissolved organic compounds. Some planktonic prokaryotic microorganisms, called "diazotrophs", use an enzyme, the nitrogenase, to fix N_2 and convert it into ammonia (NH_3) and ultimately ammonium (NH_4^+). At the global scale, they provide the major external source of reactive nitrogen to the ocean (Gruber, 2008), and support up to 50 % of new production in tropical and subtropical (LNLC) regions (Bonnet et al., 2009; Capone, 1997; Deutsch et al., 2007; Karl et al., 1997; Moutin et al., 2008; Raimbault and Garcia, 2008). These organisms are physiologically and taxonomically diverse including cyanobacteria, bacteria, and archaea (Zehr and Bombar, 2015; Delmont et al., 2018).

Autotrophic diazotrophs have been far more intensively studied than heterotrophic diazotrophs, whose contribution to global N_2 fixation remains unclear (Turk-Kubo et al., 2014; Bombar et al., 2016; Moisander et al., 2017). Autotrophic diazotrophs have been characterized both in the field and through laboratory experiments and their physiology is consequently better known (Bergman et al., 2013; Küpper et al., 2008; Mulholland and Capone, 2001, 2000; Ohki et al., 1992; Ramamurthy and Krishnamurthy, 1967; Rubin et al., 2011). Cyanobacterial (autotrophic) diazotrophs are composed of three main groups: (1) the filamentous diazotrophs including the colonial, non-heterocyst-forming *Trichodesmium*, (2) the heterocyst-forming symbionts associated with diatoms (diatom–diazotroph associations; DDAs), and (3) the unicellular cyanobacterial diazotrophs (UCYN, phylogeneticaly divided into three groups: UCYN-A, -B, and -C). It has been established that autotrophic diazotroph growth rates are typically 1 order of magnitude lower than those of non-diazotrophs (Breitbarth et al., 2008; Falcón et al., 2005; Goebel et al., 2008; LaRoche and Breitbarth, 2005). This can be related to the high energetic demand (Postgate, 1982) required to convert N_2 to NH_3 as compared to that necessary to assimilate nitrate or ammonia. This low growth rate (compared to other phytoplankton species) mainly constrains their ecological niches to nitrate-poor regions, where they can be competitive. Moreover, their geographical distribution is constrained by nutrient availability in the photic layer (mainly iron and phosphate; Berman-Frank, 2001; Bonnet et al., 2009; Mills et al., 2004; Moutin et al., 2005, 2008; Rubin et al., 2011; Rueter, 1988) and temperature (Staal et al., 2003). *Trichodesmium* sp. are present only in water where the temperature is above 20 °C (Capone, 1997; LaRoche and Breitbarth, 2005; Montoya et al., 2004), while some UCYN can be found in colder and deeper waters (Bonnet et al., 2015; Church et al., 2005; Moisander et al., 2010).

The spatial distribution and rates of N_2 fixation have been inferred at the global scale using several tools. Deutsch et al. (2007) have introduced the tracer P* which represents the excess of P relative to the standard N quota. A decrease in this tracer is then interpreted as N_2 fixation, since N_2 fixation extracts PO_4 alone. More recently, Luo et al. (2014) developed a multiple linear regression that relates N_2 fixation from the MAREDAT database (Luo et al., 2012) to environmental conditions (nutrients; sea surface temperature, SST; irradiance; mixed layer depth (MLD), etc.) in order to build a statistical model for global N_2 fixation distribution.

Numerical models have also been used as they allow us to overcome the scarcity of observations that may limit the implementation of the two previous approaches (Aumont et al., 2015; Bissett et al., 1999; Dutkiewicz et al., 2012; Krishnamurthy et al., 2009; Monteiro et al., 2011; Moore et al., 2006, 2013; Tagliabue et al., 2008). They can notably be used to investigate the spatial and temporal variability in dinitrogen fixation and to study its controlling environmental factors. In these models, N_2 fixation has been implemented in various ways. Some models use implicit parameterizations (Bissett et al., 1999; Maier-Reimer et al., 2005; Assmann et al., 2010; Aumont et al., 2015) to derive N_2 fixation from environmental conditions (mainly nitrate, phosphate, and iron concentrations; temperature; and light) without explicitly simulating any nitrogen fixing organisms. Alternatively, other models rely on the explicit descriptions of diazotrophs (Moore et al., 2004; Dunne et al., 2013) that have mainly been developed from the knowledge derived from laboratory experiments focused on *Trichodesmium* sp. (Fennel et al., 2001; Hood et al., 2001; Moore et al., 2001). Noticeably, several modelling studies have been especially focused on the role of iron in controlling the distribution of diazotrophs and N_2 fixation (Krishnamurthy et al., 2009; Moore et al., 2004, 2006; Tagliabue et al., 2008). Indeed, a realistic representation of marine iron concentrations has been stressed as a key factor to adequately simulate the habitat of diazotrophs (Monteiro et al., 2011; Dutkiewicz et al., 2012).

Moreover, among the full set of studies focusing on the spatial distribution of N_2 fixation, some studies (Berthelot et al., 2017; Bonnet et al., 2009, 2015; Garcia et al., 2007; Shiozaki et al., 2014) based on oceanographic campaigns have reported high N_2 fixation rates in the western tropical South Pacific (WTSP), which has been recently identified as a globally important hotspot of N_2 fixation with rates $> 600\,\mu mol\,N\,m^{-2}\,d^{-1}$ (Bonnet et al., 2017). Very high abundances of *Trichodesmium* have been historically reported in this region (Dupouy et al., 2000, 2011; Moisander et al., 2008; Neveux et al., 2006; Shiozaki et al., 2014; Stenegren et al., 2018) and have recently been identified as the major contributor to N_2 fixation in this region (Berthelot et al., 2017; Bonnet et al., 2018). However, the reasons for such an ecological success of diazotrophs in this region are still poorly understood.

In this study, we aim at bringing new insights into this known, but poorly understood, "N_2 fixation hotspot". This study aims to understand the spatial and temporal distribution (i.e. seasonal variability) of *Trichodesmium* and to evaluate the potential impact of *Trichodesmium* fixers on the biogeochemical conditions of the WTSP. We will specifically address the following overarching questions: (i) what are the mechanisms that structure the *Trichodesmium* distribution in the WTSP, particularly around the southwest Pacific islands, and (ii) what is the biogeochemical impact of N_2 fixation in this region? Note, this study also takes advantage of the sampling done during the "Oligotrophy to UlTra-oligotrophy PAcific Experiment" (OUTPACE), which nicely complements the data coverage in the southwest Pacific, and allows a better characterization of the processes responsible for the spatial and seasonal variability in N_2 fixation.

To fulfill our objectives, we have implemented an explicit representation of the nitrogen fixers, based on the *Trichodesmium* physiology, in a biogeochemical model. The first section of this study describes the experimental design and the observations used in our study, while the second part of the paper provides a validation of our reference simulation with an analysis of the *Trichodesmium* compartment and its impacts on the biogeochemical conditions of the tropical Pacific. In the discussion, the impact of iron from island sediment on dinitrogen fixation is considered as well as the added value of an explicit dinitrogen fixer compartment rather than a simpler implicit representation of N_2 fixation. Finally, implications for and limits of our modelling exercise are detailed in the conclusion.

2 Methods

2.1 Coupled dynamical–biogeochemical model (ROMS-PISCES)

2.1.1 ROMS

In this study, we used a coupled dynamical–biogeochemical framework based on the regional ocean dynamical model ROMS (Regional Oceanic Modeling System, (Shchepetkin and McWilliams, 2005) and a new version of biogeochemical model PISCES (Pelagic Interactions Scheme for Carbon and Ecosystem Studies). The ocean model configuration is based on the ROMS-AGRIF (Penven et al., 2006) computer code and covers the tropical Pacific region (33° S–33° N, 110° E–90° W). It has 41 terrain-following vertical levels with 2–5 m vertical resolution in the top 50 m of the water column, then 10–20 m resolution in the thermocline and 200–1000 m resolution in the deep ocean. The horizontal resolution is 1°. The turbulent vertical mixing parameterization is based on the non-local K profile parameterization (KPP) of Large et al. (1994). Open boundary conditions are treated using a mixed active/passive scheme (Marchesiello et al., 2001). This scheme is used to force our regional configuration with monthly climatological large-scale boundary conditions from a 0.5° ORCA global ocean simulation (details available in Kessler and Gourdeau, 2007), while allowing anomalies to radiate out of the domain. The use of similar ROMS configurations (e.g. vertical resolution, mixed active/passive scheme, turbulent vertical mixing parameterization) in the WTSP is largely validated through studies demonstrating skills in simulating both the surface (Jullien et al., 2012, 2014; Marchesiello et al., 2010) and subsurface ocean circulation (Couvelard et al., 2008).

To compute the momentum and fresh water and/or heat fluxes, we also use a climatological forcing strategy. Indeed, documenting the interannual to decadal variability is beyond the scope of our study, which justifies using climatological forcing fields. A monthly climatology of the momentum forcing is computed from the 1993–2013 period of the ERS1-2 scatterometer stress (http://cersat.ifremer.fr/oceanography-from-space/our-domains-of-research/air-sea-interaction/ers-ami-wind, last access: 12 July 2018). Indeed, the ERS-derived forcing has been shown to produce adequate simulations of the Pacific Ocean dynamics (e.g. Cravatte et al., 2007). A monthly climatology at 0.5° resolution computed from the Comprehensive Ocean–Atmosphere Data Set (COADS; Da Silva et al., 1994) is used for heat and fresh water forcing. In our set-up, ROMS also forces on line a biogeochemical model using a WENO5 advection scheme (i.e. five order weighted essentially non-oscillatory scheme; Shchepetkin and McWilliams, 1998). After a 1-year spin-up, we stored 1-day averaged outputs for analysis.

2.1.2 PISCES

In this study, we use a quota version of the standard PISCES model (Aumont and Bopp, 2006; Aumont et al., 2015), which simulates the marine biological productivity and the biogeochemical cycles of carbon and the main nutrients (P, N, Si, Fe). This modified model, called PISCES-QUOTA, is extensively described in Kwiatkowski et al. (2018). Our version is essentially identical to Kwiatkowski's version that included an added picophytoplankton group, except that this latter group has been removed and replaced by a *Trichodesmium* compartment. Here we only highlight the main characteristics of the model and the specifics of our model version. Our version of PISCES-QUOTA has 39 prognostic compartments. As in the standard PISCES version, phytoplankton growth is limited by the availability of five nutrients: nitrate as well as ammonium, phosphate, silicate, and iron. Five living compartments are represented: three phytoplankton groups corresponding to nanophytoplankton, diatoms, and *Trichodesmium* and two zooplankton size classes that are microzooplankton and mesozooplankton. The elemental composition of phytoplankton and non-living organic matter is variable and is prognostically predicted by

the model. On the other hand, zooplankton are assumed to be strictly homeostatic, i.e. their stoichiometry is kept constant (e.g. Meunier et al., 2014; Sterner and Elser, 2002). Nutrient uptake and assimilation as well as limitation of growth rate are modelled according to the chain model of Pahlow and Oschlies (2009). The P quota limits N assimilation which in turns limits phytoplankton growth. The phosphorus to nitrogen ratios of phytoplankton are described based on the potential allocation between P-rich biosynthesis machinery, N-rich light harvesting apparatus, a nutrient uptake component, the carbon stores, and the remainder (Daines et al., 2014; Klausmeier et al., 2004). This allocation depends on the cell size and on the environmental conditions.

Nutrients are delivered to the ocean through dust deposition, river runoff, and mobilization from the sediment. The atmospheric deposition of iron is derived from a climatological dust simulation (Tegen and Fung, 1995). The iron from sediment is recognized as a significant source (Johnson et al., 1999; Moore et al., 2004). This iron source is indeed parameterized in PISCES as, basically, a time-constant flux of dissolved iron ($2\,\mu mol\,m^{-2}\,d^{-1}$) applied over the whole sediment surface and modulated depending only on depth. A detailed description of this sedimentary source is presented in Aumont et al. (2015). The initial conditions and biogeochemical fluxes (iron, phosphorus, nitrate, etc.) at the boundaries of our domain are extracted from the World Ocean Atlas 2009 (https://www.nodc.noaa.gov/OC5/WOA09/woa09data.html, last access: 12 July 2018).

2.1.3 *Trichodesmium* compartment

For the purpose of this study, we implemented an explicit representation of *Trichodesmium* in our PISCES-QUOTA version. Therefore, as already stated, five living compartments are modelled with three phytoplankton groups (nanophytoplankton, diatoms, and *Trichodesmium*) and two zooplankton groups (microzooplankton and mesozooplankton). Similarly to nanophytoplankton, the equation of *Trichodesmium* evolution is computed as follows:

$$\begin{aligned}\frac{\partial \mathrm{Tri_C}}{\partial t} &= (1-\delta^{\mathrm{Tri}})\mu^{\mathrm{Tri}}\mathrm{Tri} - \zeta^{\mathrm{Tri}}_{\mathrm{NO_3}} V^{\mathrm{Tri}}_{\mathrm{NO_3}} - \zeta^{\mathrm{Tri}}_{\mathrm{NH_4}} V^{\mathrm{Tri}}_{\mathrm{NH_4}} \\ &\quad - m^{\mathrm{Tri}} \frac{\mathrm{Tri_C}}{K_m + \mathrm{Tri_C}} \mathrm{Tri_C} - sh \times \omega^{\mathrm{Tri}} P^2 \\ &\quad - g^Z(\mathrm{Tri})\,Z - g^M(\mathrm{Tri})\,M. \end{aligned} \quad (1)$$

In this equation, $\mathrm{Tri_C}$ is the carbon *Trichodesmium* biomass, and the seven terms on the right-hand side represent, respectively, growth, biosynthesis costs based on nitrate and ammonium, mortality, aggregation, and grazing by micro- and mesozooplankton.

In our configuration, the photosynthesis growth rate of *Trichodesmium* is limited by light, temperature, phosphorus, and iron availability. Photosynthesis growth rate of *Trichodesmium* μ^{Tri} is computed as follows:

$$\mu^{\mathrm{Tri}} = \mu_{\mathrm{FixN_2}} + \mu^{\mathrm{Tri}}_{\mathrm{NO_3}} + \mu^{\mathrm{Tri}}_{\mathrm{NH_4}}, \quad (2)$$

where $\mu_{\mathrm{FixN_2}}$ denotes growth due to dinitrogen fixation, $\mu^{\mathrm{Tri}}_{\mathrm{NO_3}}$ and $\mu^{\mathrm{Tri}}_{\mathrm{NH_4}}$ represent growth sustained by NO_3^- and NH_4^+ uptake, respectively. Moreover, a fraction of fixed nitrogen is released back to seawater, mainly as ammonia and dissolved organic nitrogen, by the simulated *Trichodesmium* compartment. Berthelot et al. (2015a) estimated this fraction to be less than 10 % when considering all diazotrophs. We set this fraction at 5 % of the total amount of fixed nitrogen. For the other nutrients (i.e. iron and phosphorus), the same fraction is also released.

Dinitrogen fixation is limited by the availability of phosphate, iron, and light and is modulated by temperature. Loss processes are natural mortality and grazing by zooplankton. Natural mortality is considered to be similar to the other modelled phytoplankton species. Grazing on *Trichodesmium* is rarely described, but it is admitted that *Trichodesmium* represents a poor source of food for zooplankton (O'Neil and Romane, 1992) especially because they contain toxins (Hawser et al., 1992). On the other hand, many species of copepods have been shown to be able to graze on *Trichodesmium* despite the strong concentrations of toxins (O'Neil and Romane, 1992). For these reasons we applied two different coefficients for the grazing preference by mesozooplankton and microzooplankton (Table 1). For microzooplankton, grazing preference is halved to account for *Trichodesmium* toxicity, and for mesozooplankton the grazing preference is similar to that of the other phytoplankton species. The complete set of equations of *Trichodesmium* is detailed in Appendix A. Table 1 presents the parameters that differ between nanophytoplankton and *Trichodesmium*.

This set-up reproduces dinitrogen fixation through an explicit representation of the *Trichodesmium* biomass (to be compared with the often used implicit parameterizations (Assmann et al., 2010; Aumont et al., 2015; Dunne et al., 2013; Maier-Reimer et al., 2005; Zahariev et al., 2008) that directly link environmental parameters to nitrogen fixation without requiring the *Trichodesmium* biomass to be simulated).

2.2 Experimental set-up

Below the set of experiments that have been performed in this study is summarized (Table 2). All climatological simulations have been run for 20 years from the same restart and only the last 19 years are considered in our diagnostics. We chose the above-described simulation explicitly modelling the *Trichodesmium* to be our reference experiment (hereafter referred to as "TRI"). In a second experiment called "TRI_NoFeSed", the model set-up is identical to the reference experiment, except that iron input from the sediments is turned off between 156° E and 120° W. In a third experiment "TRI_imp", the explicit dinitrogen fixation module is

Table 1. Models parameters for *Trichodesmium* (Tricho.) and nanophytoplakton (Nano.).

Parameters	Symbol	Units	Value	Reference
Maximum growth rate for Tricho.	μ_{max}^{Tri}	d^{-1}	0.25	Breitbarth et al. (2007)
Maximum growth rate for Nano.	μ_{max}^{Nano}	d^{-1}	1.0	
Initial slope P-I Tricho.	αI	$(W\,m^{-2})^{-1}\,d^{-1}$	0.072	Breitbarth et al. (2008) and Hood et al. (2001)
Initial slope P-I Nano.	αI	$(W\,m^{-2})^{-1}\,d^{-1}$	2.0	
Microzoo preference for Tricho.	p_{Tri}^{I}	–	0.5	
Microzoo preference for Nano.	p_{Nano}^{I}	–	1.0	
Maximum Fe / C in Tricho.	$\theta_{max,Tri}^{Fe}$	mol Fe (mol C)$^{-1}$	1×10^{-4}	Kustka et al. (2003)
Maximum Fe / C in Tricho.	$\theta_{max,Nano}^{Fe}$	mol Fe (mol C)$^{-1}$	4×10^{-5}	
Maintenance iron	m	mol Fe (mol C)$^{-1}$	1.4×10^{-5}	Kustka et al. (2003)
Maintenance use efficiency	β	mol C (mol Fe)$^{-1}$ d^{-1}	1.4×10^{-4}	Kustka et al. (2003)

Table 2. List and description of the different experiments.

Name	N_2 fixation	Iron from sediment
TRI	explicit	yes
TRI_NoFeSed	explicit	no
TRI_imp	implicit	yes
Wo_N2	no	yes

replaced by the implicit parameterization described in Aumont et al. (2015), where fixation depends directly on water temperature, nitrogen, phosphorus, and iron concentrations and light (no nitrogen fixers are simulated). Finally, a fourth experiment "Wo_N2" corresponds to a model set-up in which no explicit nor implicit description of dinitrogen fixation is activated.

Comparison between TRI and TRI_NoFeSed experiments enables us to estimate the impact of iron input from island sediments on the dinitrogen fixation, while the impact of dinitrogen fixation on the biogeochemical conditions in the Pacific Ocean can be investigated by comparing TRI and Wo_N2. Finally, the TRI and TRI_imp experiments are used to evaluate the added value of an explicit description of dinitrogen fixation relative to an implicit inexpensive parameterization.

2.3 Observational datasets

Several different databases have been used to evaluate the model skills. For nitrate and phosphate, the 0.5° global CSIRO Atlas of Regional Seas (CARS; http://www.marine.csiro.au/~dunn/cars2009/, last access: 12 July 2018) has been used. Iron has been evaluated with the global database from Tagliabue et al. (2012) complemented with the dissolved iron data from the OUTPACE cruise (Guieu et al., 2018). This database is a compilation of 13 125 dissolved iron observations covering the global ocean and encompassing the period 1978–2008. The global MARine Ecosytem DATa (MAREDAT; https://doi.pangaea.de/10.1594/PANGAEA.793246) database of N_2 fixation has been expanded with data from recent cruises performed in the WTSP: MOORSPICE (Berthelot et al., 2017), DIAPALIS (Garcia et al., 2007), NECTALIS (http://www.spc.int/oceanfish/en/ofpsection/ema/biological-research/nectalis, last access: 12 July 2018), PANDORA (Bonnet et al., 2015), OUTPACE (Bonnet et al., 2018), and Mirai (Shiozaki et al., 2014). This database contains 3079 data points at the global ocean scale, of which $\sim$ 1300 are located in our simulated region (Luo et al., 2012). Finally, we have used surface chlorophyll concentrations from the GLOBCOLOUR project (http://hermes.acri.fr, last access: 12 July 2018) which spans the 1998–2013 time period.

3 Results

3.1 Model validation

In this subsection, we aim at validating our reference simulation "TRI" with the data previously presented. In the Pacific, phosphate and nitrate concentrations show maxima in the upwelling regions, i.e. along the western American coast, and in the equatorial upwelling (Fig. 1a, c), and minima in the subtropical gyres. First, phosphate patterns show modelled values and structures in qualitatively good agreement with observations, despite an underestimation in the areas of high concentrations as within the Costa Rica dome and along the Equator. In contrast, the nitrate structure shows larger biases. We observe concentrations higher than 1 µmol L^{-1} all along the Equator in CARS, while the model nitrate concentrations are lower than this value west of 170° W. More generally the model tends to underestimate nitrate concentrations.

The regions most favourable for *Trichodesmium* can be defined by temperatures within 25–29 °C (Breitbarth et al., 2007). The model reproduces relatively well the spatial distribution of this temperature preferendum. This distribution

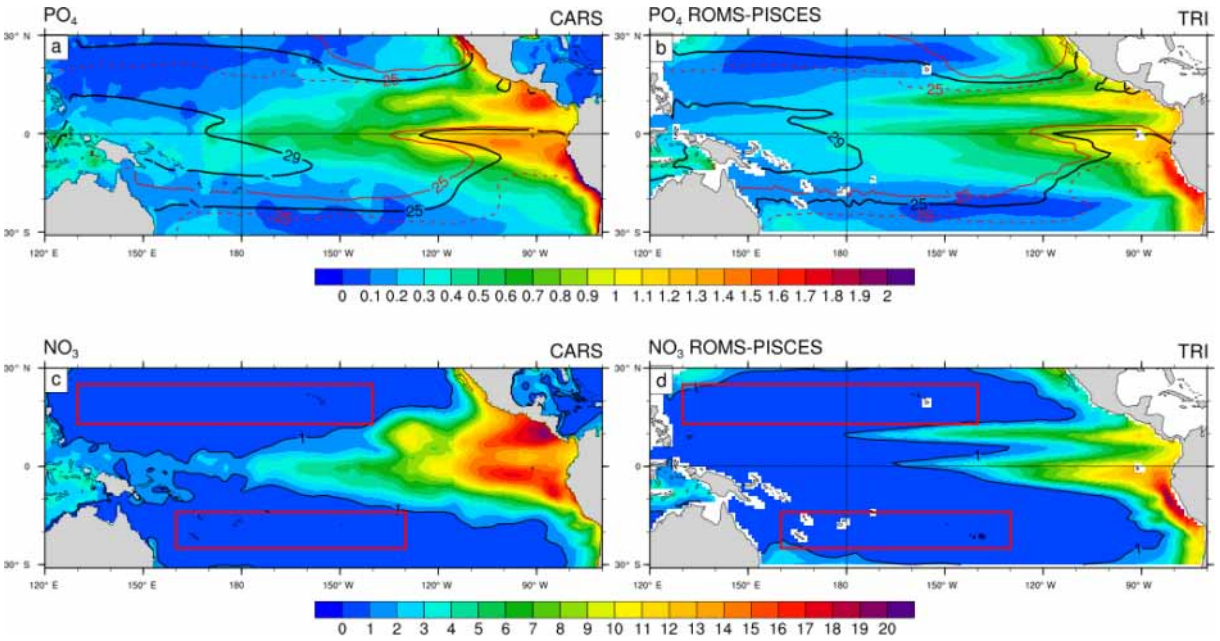

Figure 1. Annual mean concentrations in µmol L^{-1}: **(a)** PO_4 data from CARS **(b)** PO_4 simulated by the ROMS-PISCES model **(c)** NO_3 data from CARS **(d)** NO_3 simulated by the ROMS-PISCES model. On panels **(a)** and **(b)**, the black contours show the annual mean patterns of the temperature preferendum from observations **(a)** and the model **(b)**. The red contours display the 25 °C isoline in austral winter (plain) and in austral summer (dash). On panels **(c)** and **(d)** the red boxes represent the LNLC regions (defined as region where $[NO_3^-] < 1\,\mu mol\,L^{-1}$ and $[Chl] < 0.1\,mg\,Chl\,m^{-3}$).

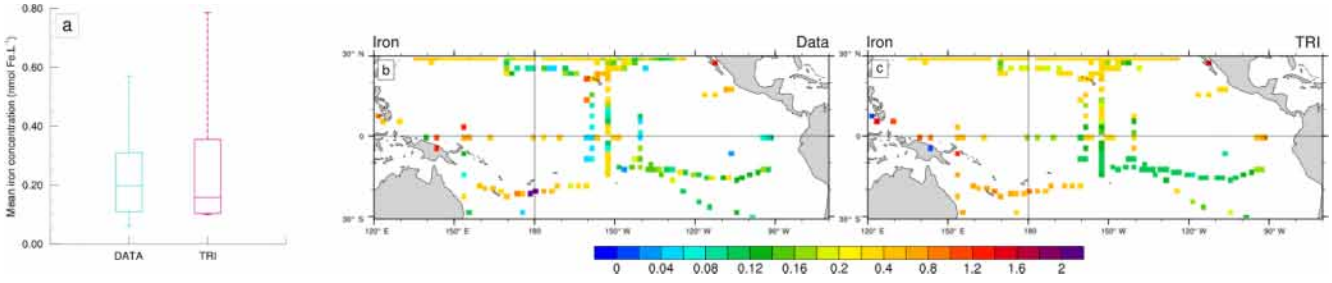

Figure 2. **(a)** Box plots of the 0–150 m averaged Iron (nmol Fe L^{-1}) data (blue) and the equivalent for the model (red) co-localized with the observations in space and time. The coloured box represents the 25–75 % quartile of the distribution, the whiskers the 10–90 % percentile distribution. The line inside the coloured box is the median. **(b, c)** Iron concentrations (nmol Fe L^{-1}) as observed **(b)** and as simulated by the model **(c)**. Iron concentrations have been averaged over the top 150 m of the ocean. Model values have been sampled at the same location, the same month, and the same depth as the data.

exhibits a significant seasonal variability, mainly as a result of the variability of the 25 °C isotherm. The latter moves by ∼ 7° latitudinally between summer and winter in the WTSP, and by ∼ 15° in the western tropical North Pacific (WTNP; Fig. 1a). This displacement is well reproduced in the TRI simulation (Fig. 1b). By contrast, along the Equator the mean position of the 25 °C isotherm is shifted eastward in the TRI simulation (120° W) compared to the observations (125° W; Fig. 1a vs. b), but its seasonal displacements are well reproduced except in the southeastern Pacific. Overall, this temporal variability is well reproduced by the model (Fig. 1b), despite this bias. In contrast, nitrate and phosphate seasonal variability remains low (not shown).

Another important feature that needs to be properly reproduced by the model is the iron distribution in the upper ocean. We have sampled the modelled values at the same time and same location as the data. The median value, as well as the dispersion of the iron surface concentrations over the tropical Pacific, are displayed for both the data and the model in Fig. 2a. The Mann–Whitney test reveals that these two normalized distributions are not significantly different (p value = 0.26). Figure 2b, c display the observed iron field and the modelled values, respectively. The best sampled area

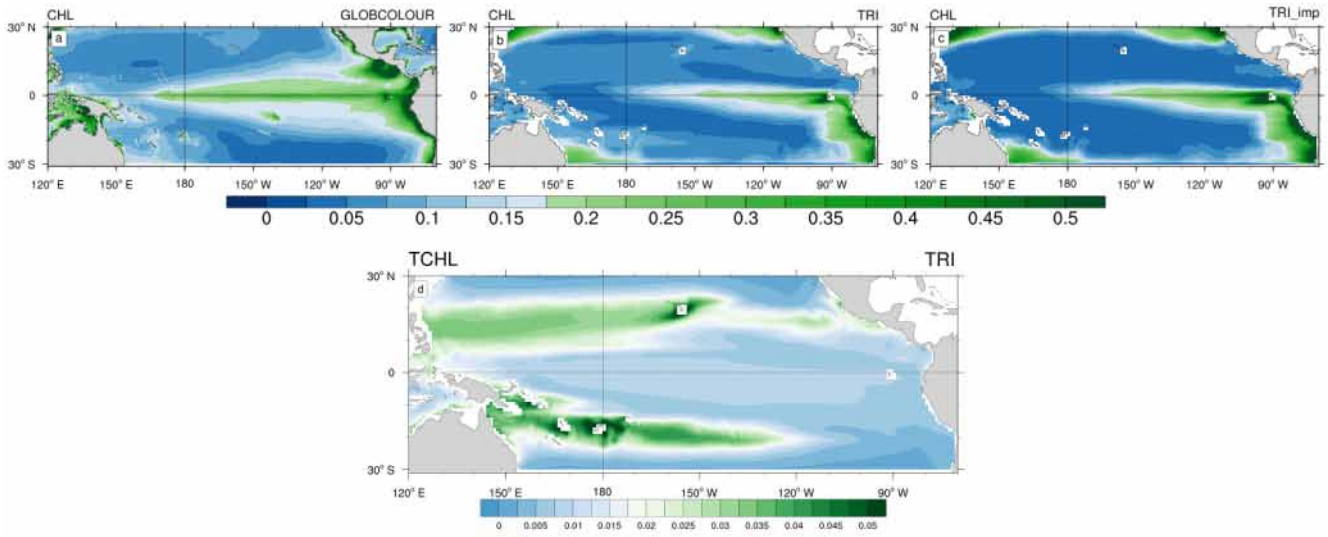

Figure 3. (a, b, c) Annual mean surface chlorophyll concentrations (in mg Chl m^{-3}) from **(a)** GLOBCOLOUR data **(b)** TRI simulation and **(c)** TRI_imp simulation. Panel **(d)** shows the annual mean surface chlorophyll concentrations of *Trichodesmium* in the TRI simulation.

is the central Pacific Ocean where simulated iron concentrations are low (0.1 to 0.3 nmol Fe L^{-1}, Fig. 2c), which is consistent with the observations (Fig. 2b). The southwest Pacific is characterized by relatively high surface iron concentrations, between 0.4 and 0.8 nmol Fe L^{-1}, both in the data and in the model. Large scale patterns are thus well represented by the model. Nevertheless, the model tends to overestimate iron levels in the South Pacific Gyre, between 180 and 140° W at about 20° S.

Figure 3 displays a comparison between surface chlorophyll (Chl) concentrations from GLOBCOLOUR data (a), from TRI (b), and TRI_imp (c) simulations. High chlorophyll concentrations are found in the eastern equatorial Pacific upwelling and along Peru in both the observations and our two simulations, with mean values higher than 0.3 mg Chl m^{-3}. However, the equatorial chlorophyll maximum simulated by the model (Fig. 3b, c) is too narrow compared to the observations, especially in the Northern Hemisphere. Similarly, the model is unable to simulate the elevated chlorophyll levels around the Costa Rica dome and the localized enhanced chlorophyll off Papua New Guinea. In TRI (Fig. 3b), chlorophyll values in the southwest Pacific region vary between 0.1 and 0.2 mg Chl m^{-3}, with maxima located in the vicinity of the Fiji and Vanuatu islands. These values are within the range of the data, even if the data tend to be slightly higher (up to 0.3 mg Chl m^{-3} near the coasts). The spatial structure is well represented, with maxima simulated around the islands. In the subtropical gyres, the simulation predicts chlorophyll concentrations of ~ 0.05 mg Chl m^{-3} which are higher than in the observations (< 0.025 mg Chl m^{-3}). In contrast to TRI_imp (Fig. 3c), chlorophyll values in the southwest Pacific and in the Northern Hemisphere are too low in comparison with the ocean colour data (Fig. 3a).

Part of the surface chlorophyll in Fig. 3b is associated with *Trichodesmium*. Figure 3d shows the annual mean spatial distribution of surface *Trichodesmium* chlorophyll in the TRI simulation. This distribution displays two zonal tongues in the tropics, one in each hemisphere. Maximum values are located in the southwest Pacific (around Vanuatu archipelago, New Caledonia, Fiji, and Papua New Guinea) and around Hawaii, where they reach 0.06 mg Chl m^{-3}. In the South Pacific, high chlorophyll biomass extends eastward until 130° W. Further east, concentrations drop to below 0.02 mg Chl m^{-3}. It is important to note that, in the observations, *Trichodesmium* have never been observed eastward of 170° W. This bias in the model could be explained by the overestimated iron concentrations in the South Pacific Gyre. In the Northern Hemisphere, between the coasts of the Philippines (120° E) and Hawaii (140° W), *Trichodesmium* chlorophyll concentrations are greater than 0.03 mg Chl m^{-3}. In the northeast Pacific, *Trichodesmium* chlorophyll is lower, yet significant (< 0.03 mg Chl m^{-3}). Otherwise the equatorial Pacific and southeast Pacific oceans are overall poor in *Trichodesmium*.

In Fig. 4, the dinitrogen fixation rates predicted by the model in TRI are compared to the observations from the MAREDAT expanded database. Evaluation of the model behaviour remains quite challenging because of the scarcity of the observations. Some large areas are not properly sampled such as the northwest tropical Pacific and the eastern Pacific. In addition, some areas are sampled only in the surface layer (0–30 m), while others have been sampled deeper. This non-homogeneous sampling may alter the distribution of the N_2 fixation rates and undermine the comparison with model outputs. To overcome this sampling bias we compared the observations with N_2 fixation rates simulated and integrated

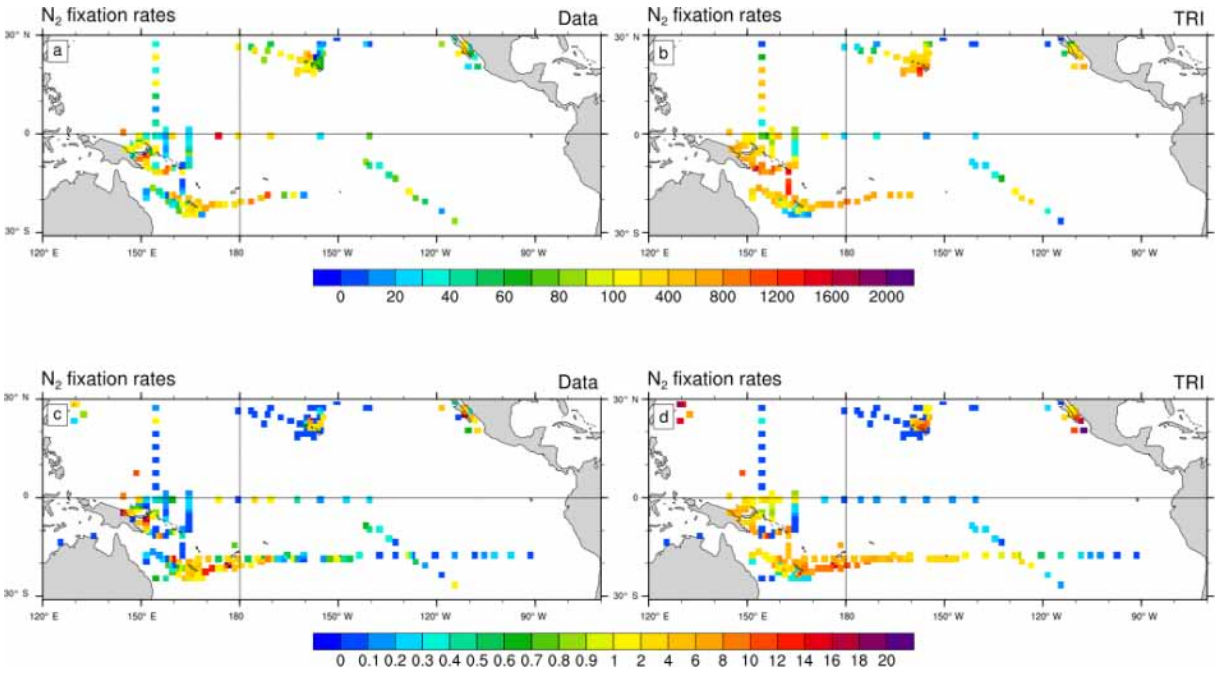

Figure 4. N_2 fixation rates (µmol N m^{-2} d^{-1}) as observed **(a, c)** and as simulated by TRI simulation **(b, d)**. In panels **(a)** and **(b)**, N_2 fixation rates have been integrated over the top 150 m of the ocean. In panels **(c)** and **(d)**, the vertical integration has been restricted to the top 30 m of the ocean. Model values have been sampled at the same location, the same month (climatological month vs. real month), and the same depth as the data.

over two different layers (0–30 and 0–150 m). Despite their scarcity, some regional patterns emerge from the observations. Maximum fixation rates (600 to 1600 µmol N m^{-2} d^{-1}; Fig. 4a) are observed around the southwest Pacific islands, in the Solomon Sea, around the Melanesian archipelagos, and around Hawaii, four well-known "hotspots" of N_2 fixation (Berthelot et al., 2015b, 2017; Bonnet et al., 2009, 2017; Böttjer et al., 2017). The modelled regional patterns of strong fixation are coherent with the observations (Fig. 4b), showing values in the same range. In the South Pacific, the TRI simulation is able to reproduce the strong east–west increasing gradient of N_2 fixation (Shiozaki et al., 2014; Bonnet et al., 2018; Fig. 4c, d). In the equatorial central Pacific, modelled values of mean fixation are negligible ($<$ 0.5 µmol N m^{-2} d^{-1}) in contrast to the observations which suggest low but non-negligible fixation rates (between 1 and 2 µmol N m^{-2} d^{-1}) (Bonnet et al., 2009; Halm et al., 2012). On the whole modelled domain, and for both integration layers, dinitrogen fixation rates are overestimated by 70 % in TRI compared to the data. Some recent studies have shown that the $^{15}N_2$ tracer addition method (Montoya et al., 2004) used in most studies reported in the MAREDAT database may underestimate N_2 fixation rates due to an incomplete equilibration of the $^{15}N_2$ tracer in the incubation bottles. Thus, this overestimation may be an artifact arising from methodological issues (Großkopf et al., 2012; Mohr et al., 2010). However, some other studies performed in the South Pacific (Bonnet et al., 2016b; Shiozaki et al., 2015) compared the two methods, and did not find any significant differences.

3.2 *Trichodesmium* primary production

We evaluated the direct relative contribution of *Trichodesmium* to primary production (PP; Fig. 5). The spatial distribution of this contribution is very similar to the spatial distribution of *Trichodesmium* chlorophyll, with two distinct tongues located on each side of the Equator in the tropical domain. In the Northern Hemisphere, the tongue extends from the coast of the Philippines (120° E) to Hawaii (140° W) longitudinally and between 10 and 25° N latitudinally. The maximum contribution (35 %) is reached near Hawaii while in the rest of the tongue, values are close to 20 %. In the Southern Hemisphere, the region of elevated contribution extends from PNG (140° E) to about the centre of the South Pacific subtropical gyre at 130° W, and between 5 and 25° S latitudinally. Maximum values are predicted in the vicinity of Vanuatu and Fiji Islands, where they can reach 35 %. Part of this elevated contribution is explained by the very low PP rates simulated in this region for both nanophytoplankton and diatoms (less than 0.03 mol C m^{-3} yr^{-1}). Furthermore, the island effect seems to represent an important factor for explaining the spatial distribution of *Trichodesmium* growth rates. Indeed, maximum *Trichodesmium* chlorophyll concentrations and the largest contribution of *Trichodesmium* to PP are achieved near the islands. Finally, in LNLC regions (red

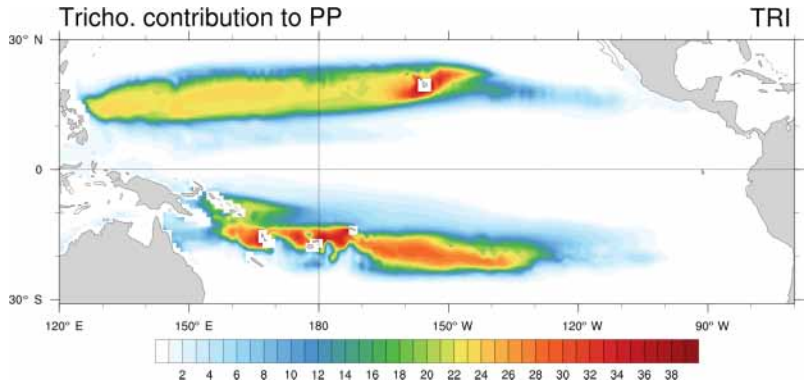

Figure 5. Relative contribution (in percentage) of *Trichodesmium* to total primary production.

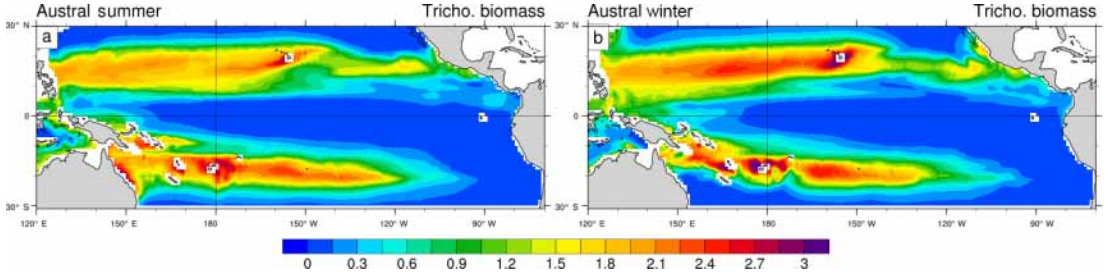

Figure 6. *Trichodesmium* biomass (mmol C m^{-2}) in **(a)** austral summer and **(b)** austral winter, integrated over the top 100 m of the ocean.

boxes; Fig. 1c, d), we assess that *Trichodesmium* contribute to 15 % of total PP, which is in accordance with biogeochemical studies performed in these areas (Bonnet et al., 2015; Berthelot et al., 2017; Caffin et al., 2018).

3.3 Seasonal variability in *Trichodesmium* biomass

Trichodesmium biomass (Fig. 6) and simulated dinitrogen fixation rates (Fig. 7) display a seasonal variability that is driven by the seasonal variability of the environmental conditions (light, temperature, currents, nutrients). The regional maxima of *Trichodesmium* biomass (exceeding 3 mmol C m^{-2}; integrated over the top 100 m of the ocean) are found in both hemispheres during the summer season (Fig. 6a, b) even if locally, maxima can be attained during other periods of the year than summer. In the South Pacific, the area of elevated *Trichodesmium* biomass moves by 3° southward from austral winter to austral summer. Along Australia and in the Coral Sea, *Trichodesmium* biomass exhibits a large seasonal variability with a very low winter biomass that contrasts with elevated values in summer. A similar important variability, which is shifted by 6 months, is simulated in the Northern Hemisphere in the Micronesia region and in the Philippine Sea.

Unfortunately, due to the scarcity of N_2 fixation data, this seasonal cycle cannot be properly assessed at the scale of the tropical Pacific Ocean. This is only feasible at the time series station ALOHA located in the North Pacific Gyre at 22°45′N, 158° W, where seasonal data of dinitrogen fixation are available from 2005 to 2012 (Böttjer et al., 2017). They proved that vertically integrated dinitrogen fixation rates are statistically significantly (one-way ANOVA, $p < 0.01$) lower from November to March (less than 200 µmol N m^{-2} d^{-1}) than from April to October (about 263 ± 147 µmol N m^{-2} d^{-1}) as highlighted in Fig. 7a (blue dots). In the model (red dots; Fig. 7a), the maximum amplitude of the seasonal cycle appears to be underestimated relative to the observations (i.e. respectively ~ 170 and ~ 250 µmol N m^{-2} d^{-1}). Dinitrogen fixation peaks 1 month earlier in the model than in the data (August for the model and September for the data). Indeed, the simulated dinitrogen fixation rates are minimum between December and May (averaging $\sim 241 \pm 27$ µmol N m^{-2} d^{-1}) and maximum the rest of the year (averaging $\sim 347 \pm 52$ µmol N m^{-2} d^{-1}). These values are comparable to the data even if they are slightly higher.

In order to assess the seasonal cycle of N_2 fixation rates in the South Pacific (red box Fig. 1c; 160–230° E, 25–14° S), we have extracted the available data for each month from our database (blue dots; Fig. 7b), and the corresponding model values in TRI (red dots; Fig. 7b). In July no observations are available and in January, April, and August only one data point is available for the entire region. The predicted seasonal cycle is broadly consistent with the observations. Minimum dinitrogen fixation rates (239 ± 205 µmol N m^{-2} d^{-1}) occur during austral winter and autumn. Maximum rates are reached in February and March, where they exceed

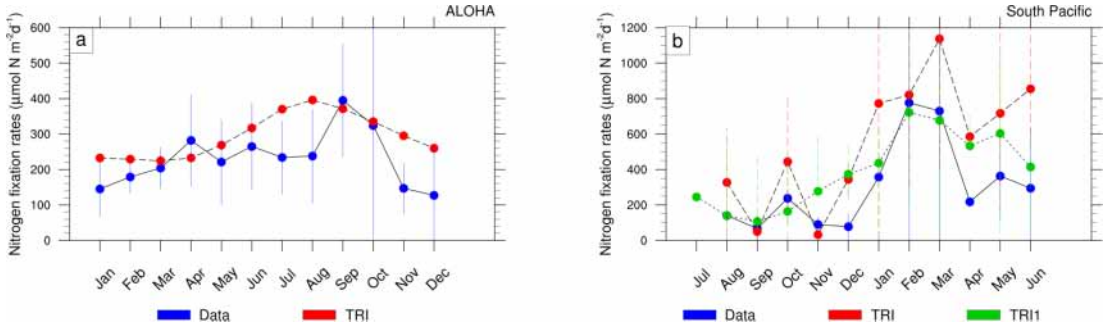

Figure 7. (a) Depth-integrated (0 to 125 m) rates of N_2 fixation ($\mu mol\,N\,m^{-2}\,d^{-1}$) at ALOHA for the data (blue) and TRI simulation (red). **(b)** Depth-integrated (from 0 to 150 m) rates of N_2 fixation ($\mu mol\,N\,m^{-2}\,d^{-1}$) in the South Pacific (red box, Fig. 1c) in the data (blue) and in the TRI simulation (red). The blue curve is the average of all the model points inside the South Pacific zone (red box, Fig. 1c), whereas the green curve corresponds to the average of the model points where data are available.

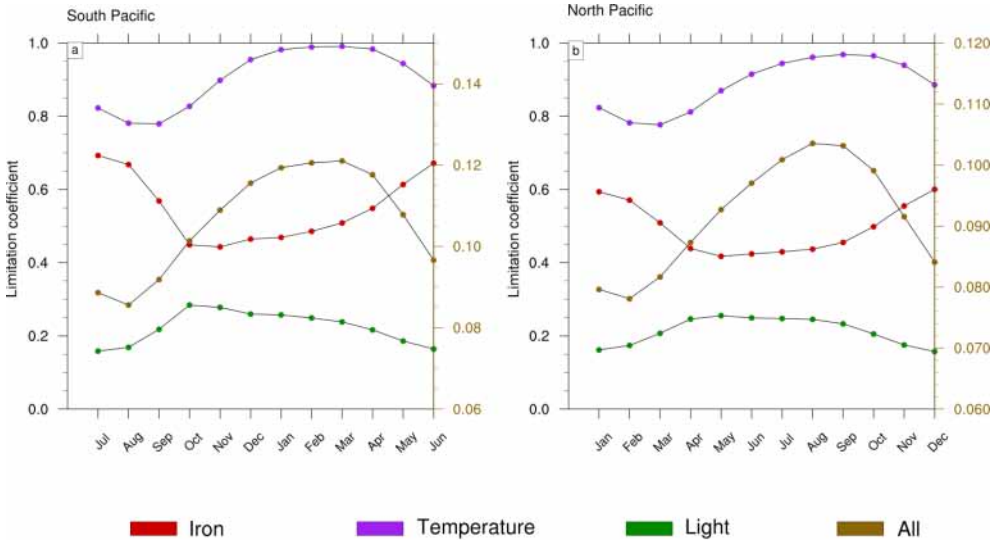

Figure 8. Seasonal cycle of the limitation terms of *Trichodesmium* production in **(a)** the South Pacific and **(b)** the North Pacific. The right scale (in brown) represents the total limitation.

$600\,\mu mol\,N\,m^{-2}\,d^{-1}$ in the observations. The increase in dinitrogen fixation rates occurs 1 month earlier than in the observations, in December instead of January, and remains 2 to 3 fold higher from April to June. It is important to note here that the sampling spatial and temporal distribution may distort the seasonal cycle. Using the model, it is possible to evaluate how well the seasonal cycle is captured by the sampling (red dots compared to green dots; Fig. 7b). The general structure of the seasonal cycle remains relatively unaltered. However, the amplitude is significantly impacted since it reaches $1100\,\mu mol\,N\,m^{-2}\,d^{-1}$ if sampled at the observed stations, whereas it is about twice as low at $600\,\mu mol\,N\,m^{-2}\,d^{-1}$ if all the model data points are considered. We can conclude that the TRI simulation reproduces well the seasonal cycle of N_2 fixation rates at the Pacific scale, even though more data are needed to improve the evaluation of the model skills.

To further investigate the mechanisms that drive the seasonal variability in *Trichodesmium* in the Pacific, we examined the factors that control *Trichodesmium* abundance in the TRI simulation (not shown). This decomposition shows that the physical terms (advection and mixing) are negligible compared to biological terms. In addition, the seasonal cycles of grazing and mortality are in phase with the production terms but their sign is opposite. In conclusion, this analysis indicates that this seasonal variability is mainly controlled by the levels of PP, the other terms of tracer evolution dampen its amplitude but do not change its shape. Hence we further examine the limitation terms of PP (Fig. 8) in two representative regions characterized by elevated levels of N_2 fixation rates (red boxes; Fig. 1c). A detailed description of these limitation terms is given in Appendix A. A limitation term reaching 1 means that growth is not limited, whereas a limitation term equal to 0 means that growth ceases.

Trichodesmium growth sustained by nitrate and ammonia is very slow in LNLC regions due to their very low availability and is therefore not considered further. Thus, our analysis is restricted to dinitrogen fixation. *Trichodesmium* growth can be limited by iron and phosphate and is inhibited when reactive nitrogen (nitrate and ammonia) is available. In the WTSP, the model suggests that iron is the sole nutrient that modulates *Trichodesmium* growth (red curve; Fig. 8a, b). The other limiting factors of *Trichodesmium* growth are light (green curve; Fig. 8a, b) and temperature (purple curve; Fig. 8a, b). The product of these three limiting factors gives the limiting coefficient of dinitrogen fixation (brown curve; Fig. 8a, b). The limiting factors vary according to the season and the hemisphere. In the South (North) Pacific, temperature and light are less limiting during the austral summer (winter) than during the austral winter (summer). The limiting factor associated with temperature varies from 0.8 to 1, and the light limiting factor varies from 0.15 to 0.3. Unlike light and temperature, iron is less (more) limiting in the South (North) Pacific during winter (summer) than during the austral summer (winter) with values varying between 0.4 and 0.7. Finally, *Trichodesmium* growth is more limited during austral winter (summer) in the South (North) Pacific. The seasonal variability is forced by light and temperature, and iron mitigates its amplitude. Indeed, nutrients and iron inputs brought to the euphotic zone by the seasonally enhanced vertical mixing are counterbalanced by the related inputs (e.g. temperature) of these water masses.

4 Discussion

4.1 Impact of iron from island sediments

Monteiro et al. (2011) performed a sensitivity study and found that a 5-fold increase in the solubility of aeolian iron improves the biogeographical distribution of N_2 fixation in the southwest Pacific. In the meantime, a recent study has challenged this view by showing no increase in N_2 fixation in response to increased dust deposition (Luo et al., 2014). In any cases, the sedimentary and hydrothermal sources were not taken into account in those studies, although they are likely significant sources (Bennett et al., 2008; Johnson et al., 1999; Moore et al., 2004; Tagliabue et al., 2010; Toner et al., 2009). In parallel, Dutkiewicz et al. (2012) evaluated the sensitivity of the biogeographical distribution of N_2 fixation to the aeolian source of iron in a model which takes into account the iron sediment supplies, and conclude for minor changes in the southwest Pacific, while in the North Pacific the change was larger. Indeed, there are many islands with a marked orography that could deliver significant amounts of iron to the ocean (Radic et al., 2011) in the southwest Pacific.

To assess the impact of the sediment source of iron on the *Trichodesmium* production, we used the "TRI_NoFeSed" experiment in which this specific source of iron has been turned off for the islands between 156° E and 120° W (Table 2). In this simulation, iron and *Trichodesmium* chlorophyll decrease by 58 and 51 %, respectively (Fig. 9a, b), in the WTSP (red box Fig. 1c). Figure 9c displays the iron distribution simulated in TRI_NoFeSed, and shows that the maxima around the islands disappear. Furthermore, in the South Pacific, iron decreases due to the reduction of the zonal advection of iron downstream of the islands. The iron flux from the sediments around the islands also affects the spatial structure of *Trichodesmium* chlorophyll (Fig. 9e, f), most noticeably in the South Pacific, with maxima shifted from the South Pacific islands region (e.g. Fiji, New Caledonia, Vanuatu) in the TRI simulation to the coastal regions near Australia and Papua New Guinea in the TRI_NoFeSed simulation. In the Northern Hemisphere, the effects of the sediment flux of iron are less important with a shift of the *Trichodesmium* chlorophyll maxima towards the Philippine Sea and a localized effect near Hawaii. This sensitivity test demonstrates that *Trichodesmium* are highly sensitive to the iron distribution in our model and hence that the spatial patterns of *Trichodesmium* chlorophyll in the southwest Pacific are tightly controlled by the release of iron from the coastal sediments of the Pacific islands.

4.2 *Trichodesmium* impacts on biogeochemistry

One of the questions we want to address is the quantification of the *Trichodesmium* impact on PP, at the Pacific scale with a focus on the WTSP region. In the oligotrophic waters of the South Pacific, dinitrogen fixation can be an important source of bio-available nitrogen in the water column through *Trichodesmium* recycling which can feed other phytoplankton. To evaluate that impact, we calculated the relative increase in PP between the TRI simulation and the Wo_N2 simulation in which no N_2 fixation is considered (Fig. 10a). As expected, the spatial structure of the PP differences between both simulations matches the N_2 fixation spatial distribution in the TRI simulation (two tongues, one in each hemisphere). In the North Pacific the maximum increase in the PP due to the N_2 fixation is located around Hawaii, where it exceeds 120 %. In the remaining part of the Northern Hemisphere tongue, PP increases by 50 to 100 %. In the Southern Hemisphere, values are more homogeneous in the tongue (from 80 to 100 %), even though there is a local maximum around Fiji and Vanuatu (up to 120 %). Out of these northern and southern tongues, the increase in PP is less than 20 %. In average on our domain, the increase in PP is 19 %, and in LNLC regions it reaches approximately 50 %.

From total PP only, it is not possible to disentangle the increase in PP directly due to *Trichodesmium* themselves and the indirect increase due to the impact of N_2 fixation on the other phytoplankton groups (nanophytoplankton and diatoms). Indeed, as mentioned in the Methods section, *Trichodesmium* also releases a fraction of the recently fixed N_2 as bio-available nitrogen (in our model *Trichodesmium* re-

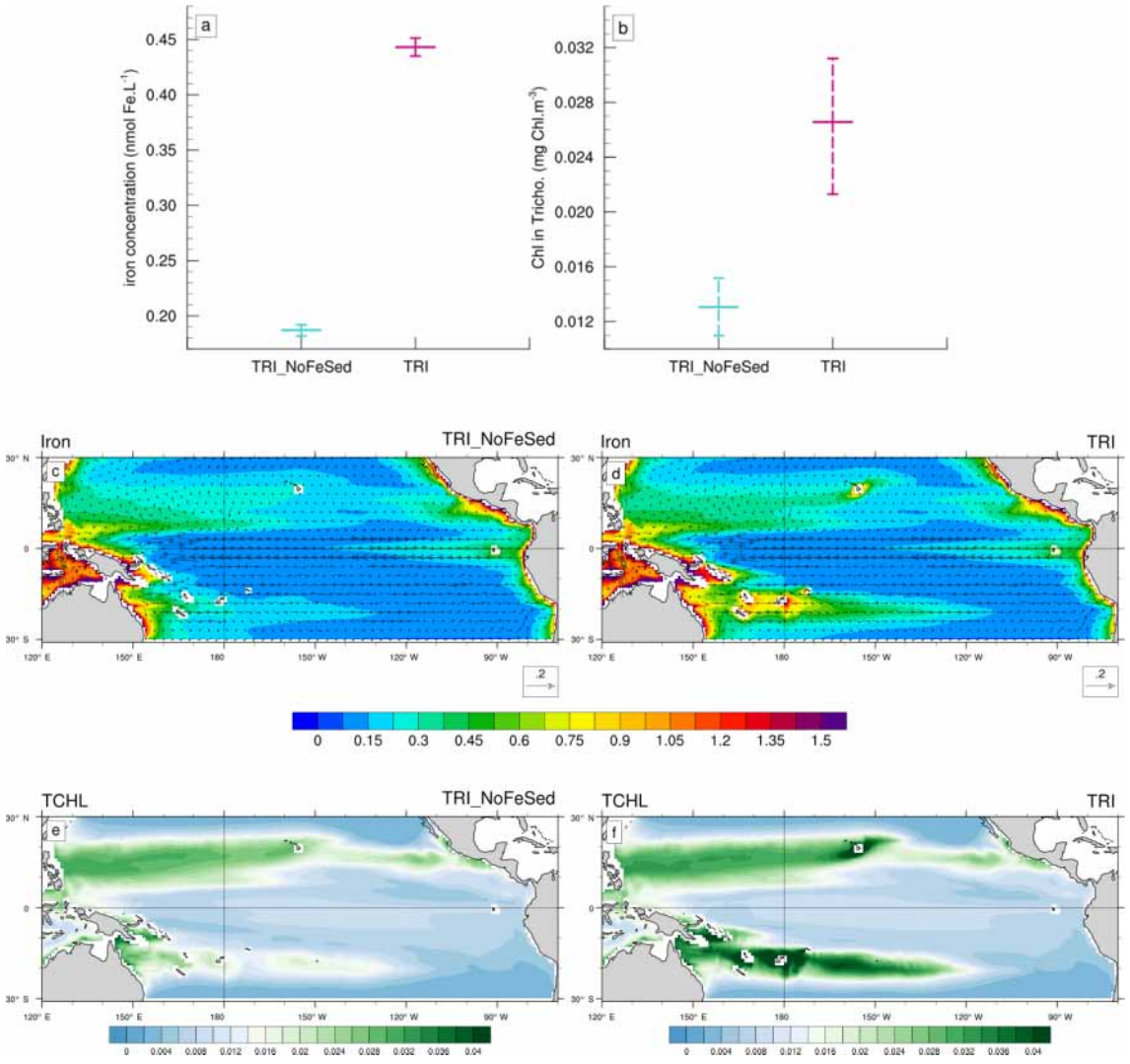

Figure 9. **(a, b)** Minimum, mean and maximum in the South box (Fig. 1c) of **(a)** the iron concentrations (in nmol Fe L^{-1}), and **(b)** of the chlorophyll concentrations of *Trichodesmium* (in mg Chl m^{-3}). **(c, d, e, f)** Annual mean iron concentrations (shading; in nmol Fe L^{-1}) and current velocities (vectors; in m s^{-1}) for **(c)** the TRI_NoFeSed simulation and **(d)** the TRI simulation. Annual mean chlorophyll concentrations of *Trichodesmium* (mg Chl m^{-3}) for **(e)** the TRI_NoFeSed simulation and **(f)** the TRI simulation. The concentrations have been averaged over the top 100 m of the ocean. The current velocities are identical on the panels **(a)** and **(b)**.

leases ammonia and dissolved organic nitrogen, but only ammonia is directly bio-available). Figure 10b displays the difference in PP due to diatoms and nanophytoplankton only. The main large-scale patterns constituted of the northern and southern tongues persist, but the intensity of the differences contrasts with those found when considering total PP (Fig. 10a). Indeed, the increase in total PP (Fig. 10a) in those two tongues is twice as high as when the direct effect of *Trichodesmium* is excluded. This analysis stresses the importance of the bio-available nitrogen released by diazotrophs as we attribute about half of the total production increase to this release. Indeed, recent isotopic studies tracing the passage of diazotroph-derived nitrogen into the planktonic food web reveal that part of the recently fixed nitrogen is released to the dissolved pool and quickly taken up (24–48 %) by surrounding planktonic communities (Berthelot et al., 2016; Bonnet et al., 2016b, a).

With the simulation TRI_imp, we aim at comparing an implicit N_2 fixation formulation to the explicit formulation used in TRI. Figure 10c displays the relative change of total PP between the TRI and the TRI_imp simulations (see Table 2). The implicit formulation displays a similar spatial distribution to that of the explicit distribution but it is predicting a lower total PP, especially in the southern Pacific where explicit formulation leads to an increase of about 45 % in total PP compared to the one related to the implicit formulation. On average across our domain, total PP is about 9 % higher

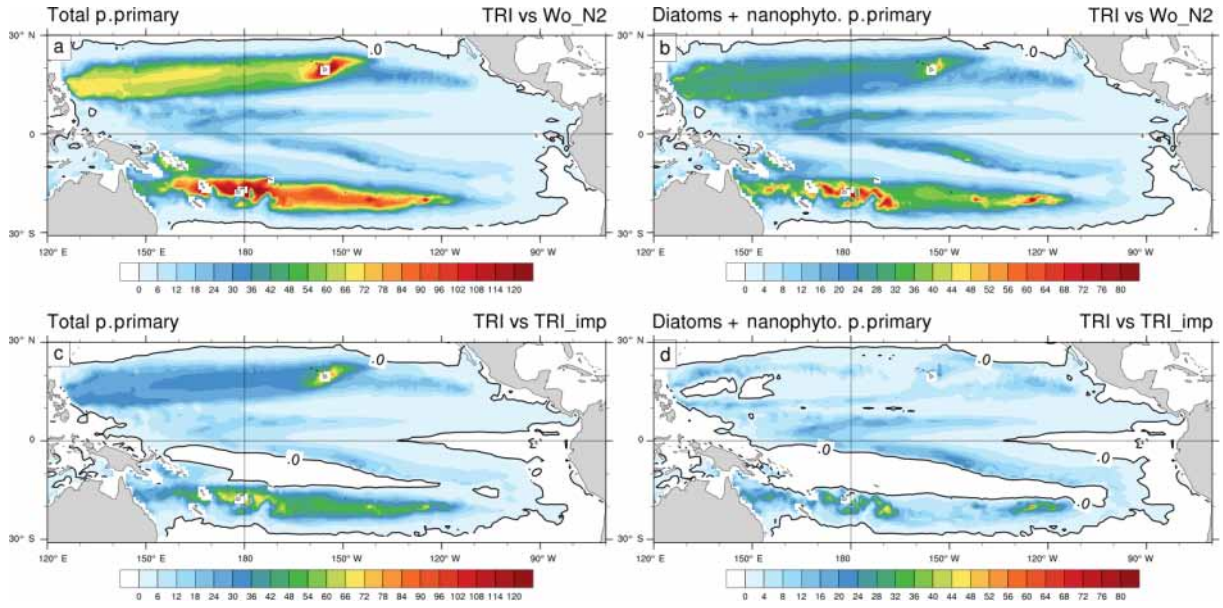

Figure 10. Percentage increase in primary production between the TRI simulation and the Wo_N2 simulation **(a, b)** and the TRI_imp simulation **(c, d)**; panels **(a)** and **(c)** show total primary production including the contribution of *Trichodesmium* whereas in panels **(b)** and **(d)**, primary production only includes the contribution of diatoms and nanophytoplankton.

when nitrogen fixation is explicitly modelled relative to an implicit formulation.

This difference becomes even weaker (2 %) if only PP by nanophytoplankton and diatoms is considered, with noticeable differences restricted to the areas of maximum N_2 fixation in the Southern Hemisphere (around the islands). PP sustained by the release of bio-available nitrogen is thus similar in the TRI and TRI_imp simulations, but an explicit representation of N_2 fixation allows for a better description of N_2 fixation patterns. Indeed, the areas of intense N_2 fixation rates cannot be properly simulated in the vicinity of the islands, especially in the Southern Hemisphere, by the tested implicit parameterization. We also assessed the carbon export (under the euphotic layer, mmol C s^{-2} d^{-1}; Fig. S1 in the Supplement) and the N_2 fixation rate (integrated over the top to 150 m; Fig. S2: panel (a) in µmol N m^{-2} d^{-1} and panel (b) in percentage) difference between TRI and TRI_imp simulations. We observe a carbon export greater in the TRI simulation, the average across the Pacific of this difference is 0.1 mmol C m^{-2} d^{-1} or 4 %, and in LNLC regions the increase varies between 6 and 10 %. The N_2 fixation rates are greater in TRI simulation except in the warm pool, in the equatorial upwelling, and in the Peruvian upwelling.

4.3 Limitations of the present study

In this study, we simulate N_2 fixation through the explicit representation of only one type of diazotrophs, the *Trichodesmium* sp. This choice has been motivated by evidences that it represents one of the main nitrogen fixers in the western tropical Pacific (Bonnet et al., 2015; Dupouy et al., 2011; Shiozaki et al., 2014) and by the relatively good knowledge (compared to other dinitrogen fixers) we have about its physiology (Ramamurthy and Krishnamurthy, 1967; Ohki et al., 1992; Mulholland and Capone, 2000; Mulholland et al., 2001; Küpper et al., 2008; Rubin et al., 2011; Bergman et al., 2013). However, our model remains simple and some of the mechanisms that drive the behaviour of *Trichodesmium* have not been implemented in our model. As an example, the ability of *Trichodesmium* to group in colonies and to vertically migrate (Kromkamp and Walsby, 1992; Villareal and Carpenter, 2003; Bergman et al., 2013) is well documented. The reason for these mechanisms remains unclear, but several hypotheses have been put forward such as avoiding nitrogenase exposition to di-oxygen (Carpenter, 1972; Gallon, 1992; Paerl et al., 1989), or maximizing light (on the surface) and nutrient (at depth) acquisition (Letelier and Karl, 1998; Villareal and Carpenter, 1990; White et al., 2006), or even increasing the efficiency of the uptake of atmospheric iron (Rubin et al., 2011). Our model does not represent those processes nor does it model the resulting vertical migration of *Trichodesmium*. Moreover, the release of fixed dinitrogen as reactive nitrogen bioavailable to other phytoplanktonic organisms has been set to a constant value of 5 %. This percentage is known to be highly variable and therefore this value is in the lowest range of the observations. An increase in this value would increase the PP due to nanophytoplankton and diatoms in the TRI simulation, and thus decrease the relative contribution of *Trichodesmium* to total PP, which would be closer to the last observations (Berthelot et al., 2017; Bonnet et al., 2017).

Some studies, mostly based on extrapolated in situ data, aimed at assessing the potential of N_2 fixation at global or regional scale (Codispoti et al., 2001; Deutsch et al., 2001; Galloway et al., 2004). In the south western tropical Pacific, Bonnet et al. (2017) have estimated total N_2 fixation at 15 to 19 Tg N yr^{-1}. For the same region, N_2 fixation is predicted to amount to ~ 7 Tg N yr^{-1} in the TRI simulation. As already mentioned, this rather low predicted estimate might be explained by the sole representation of *Trichodesmium* as nitrogen fixing organisms, which dominate in the western tropical South Pacific (Dupouy et al., 2011; Stenegren et al., 2018). It has to be noted that other diazotroph groups such UCYN-B and DDAs are abundant in the WTSP, representing 10–20 % of the overall diazotroph community (Stenegren et al., 2018). Moreover, the contribution of heterotrophic diazotrophic organisms is poorly studied and may account for a significant fraction of N_2 fixation (Moisander et al., 2017). Our model estimation has also been computed from monthly averages and is thus not taking into account the high-frequency variability that may explain at least some of the very high rates of N_2 fixation found in the study by Bonnet et al. (2017). Our assessment based on a model could thus be seen as a lower limit for N_2 fixation in the western tropical Pacific. Moreover, our model also shows a good qualitative agreement with the studies based on observations that focus on the impact of N_2 fixation in tropical oligotrophic waters (Raimbault and Garcia, 2008; Shiozaki et al., 2013). Indeed, in agreement with those studies, our reference simulation predicts that diazotrophs support a significant part of total PP (15 %) in LNLC regions.

5 Conclusion

This study describes the spatial and temporal distribution of *Trichodesmium* at the scale of the tropical Pacific Ocean, and investigates the impact of a major diazotroph species (e.g. *Trichodesmium* sp.) on the biogeochemistry of this region. Towards this end, we performed a first 20-year simulation with the coupled 3-D dynamical–biogeochemical model ROMS-PISCES in which we embedded an explicit representation of N_2 fixation based on *Trichodesmium* physiology. This simulation was shown to be able to reproduce the main physical (SST) and biogeochemical (nutrient) conditions of the tropical Pacific Ocean. This includes the spatial distribution of surface chlorophyll and N_2 fixation.

The validation of this simulation allows us to confidently assess the *Trichodesmium* distribution. The model predicts that areas favourable to *Trichodesmium* growth extend from 150° E to 120° W in the South Pacific, and from 120° E to 140° W in the North Pacific, with local optimal conditions around the islands (i.e. Hawaii, Fiji, Samoa, New Caledonia, Vanuatu). This broadly corresponds to the LNLC regions where *Trichodesmium* are predicted to be responsible for 15 % of total primary production (PP). The seasonal variability of the *Trichodesmium* habitat is dominantly controlled by SST and light, while iron availability modulates the amplitude of the seasonal cycle.

In our study we also assess the role played by iron released from the island sediments, and show that this iron source partly controls the spatial structure and the abundance of *Trichodesmium* in the western tropical South Pacific. However, this region is in the centre of the South Pacific Convergence Zone, which is the largest convective area of the Southern Hemisphere, with rainfall exceeding 6 mm d^{-1}, hence it would be interesting to assess the impact of river iron supply on the diazotroph activity. In addition, the Vanuatu archipelago and Tonga are located on the ring of fire, hence hydrothermal sources could have a strong impact on N_2 fixation. These two iron sources are not yet implemented in our configuration but may improve simulations of N_2 fixation in the southwestern tropical Pacific region. Finally, our explicit simulation of N_2 fixation has proven to be higher by 25 % (while still in the lower end of estimations from observations) than the more commonly used implicit parameterization.

Data availability. Data are available upon request.

Appendix A

Trichodesmium preferentially fixes N_2 at temperatures between 20–34 °C (Breitbarth et al., 2007). The temperature effect on the growth rate is modelled using a 4th order polynomial function (Ye et al., 2012):

$$L_T^{\mathrm{Tri}} = \left(2.32\times10^{-5}\times T^4 - 2.52\times10^{-3}\times T^3 + 9.75\times10^{-2}\times T^2 - 1.58\times T + 9.12\right)\Big/ 0.25, \quad \text{(A1)}$$

where $0.25\,\mathrm{d}^{-1}$ is the maximum observed growth rate (Breitbarth et al., 2007). Hence, at 17 °C the growth rate is zero and maximum growth rate is reached at 27 °C. The *Trichodesmium* light limitation is similar to nanophytoplankton (Aumont et al., 2015).

From Eq. (2), we distinguish two cases for the growth rate due to N_2 fixation.

If phosphorus is limiting, Eq. (2) becomes

$$\mu_{\mathrm{FixN_2}} = \mu_{\max}^{\mathrm{Tri}} \cdot L_{\mathrm{I}}^{\mathrm{Tri}} \cdot L_{\mathrm{P}}^{\mathrm{Tri}} - (\mu_{\mathrm{NO_3}}^{\mathrm{Tri}} + \mu_{\mathrm{NH_4}}^{\mathrm{Tri}}) \text{ with} \quad \text{(A2a)}$$

$$L_{\mathrm{P}}^{\mathrm{Tri}} = \min\left(1, \max\left(0, \frac{(\theta^{\mathrm{P}} - \theta_{\min}^{\mathrm{P}})\times\theta_{\max}^{\mathrm{P}}}{(\theta_{\max}^{\mathrm{P}} - \theta_{\min}^{\mathrm{P}})\times\theta^{\mathrm{P}}}\right)\right). \quad \text{(A2b)}$$

If iron is limiting,

$$\mu_{\mathrm{FixN_2}} = \mu_{\max}^{\mathrm{Tri}} \cdot L_{\mathrm{I}}^{\mathrm{Tri}} \cdot L_{\mathrm{Fe}}^{\mathrm{Tri}} - (\mu_{\mathrm{NO_3}}^{\mathrm{Tri}} + \mu_{\mathrm{NH_4}}^{\mathrm{Tri}}) \text{ with} \quad \text{(A3a)}$$

$$L_{\mathrm{Fe}}^{\mathrm{Tri}} = \min\left(1, \max\left(0, \frac{(\theta^{\mathrm{Fe}} - \theta_1^{\mathrm{Fe}})\times\theta_{\mathrm{opt}}^{\mathrm{Fe}}}{(\theta_{\mathrm{opt}}^{\mathrm{Fe}} - \theta_0^{\mathrm{Fe}})\times\theta^{\mathrm{Fe}}}\right)\right). \quad \text{(A3b)}$$

In Eq. (A3b), θ_1^{Fe} and θ_0^{Fe} are computed as follows :

$$\theta_1^{\mathrm{Fe}} = \theta_0^{\mathrm{Fe}} + \alpha\cdot\mu_{\mathrm{FixN_2}}, \quad \text{(A4a)}$$

$$\theta_0^{\mathrm{Fe}} = \theta_{\min}^{\mathrm{Fe}} + m, \quad \text{(A4b)}$$

$$\alpha = \frac{1}{\beta}, \quad \text{(A4c)}$$

where $\theta^{\mathrm{Nutrients}}$ represents the nutrient quota for iron and phosphorus (i.e. the ratio between iron and carbon concentrations in *Trichodesmium*, for instance). $\theta_{\min}^{\mathrm{P}}$ and $\theta_{\mathrm{opt}}^{\mathrm{Fe}}$ are constants, whereas $\theta^{\mathrm{Nutrients}}$ varies with time. The minimum between $L_{\mathrm{Fe}}^{\mathrm{Tri}}$ and $L_{\mathrm{P}}^{\mathrm{Tri}}$ defines the limiting nutrient. $L_{\mathrm{I}}^{\mathrm{Tri}}$ is the limiting function by temperature and light. m is the difference between the maintenance iron (i.e. the intracellular Fe : C present in the cell at zero growth rate) for a diazotrophic growth and a growth on ammonium (Kustka et al., 2003). β is the marginal use efficiency and equals the moles of additional carbon fixed per additional mole of intracellular iron per day (Raven, 1988; Sunda and Huntsman, 1997). The demands for iron in phytoplankton are for photosynthesis, respiration, and nitrate/nitrite reduction. Following Flynn et al. (1997), we assume that the rate of synthesis of new components requiring iron by the cell is given by the difference between the iron quota and the sum of the iron required by these three sources of demand, which we defined as the actual minimum iron quota:

$$\theta_{\min}^{\mathrm{Fe}} = \frac{0.0016}{55.85}\theta_{\mathrm{Tri}}^{\mathrm{Chl}} + \frac{1,21.10^{-5}\times14}{55.85\times7.625}L_{\mathrm{N}}^{\mathrm{Tri}}\times1.5 + \frac{1.15\times10^{-4}\times14}{55.85\times7.625}L_{\mathrm{NO_3}}^{\mathrm{Tri}}. \quad \text{(A5)}$$

In this equation, the first right-hand side term corresponds to photosynthesis, the second term corresponds to respiration, and the third term estimates nitrate and nitrite reduction. The parameters used in this equation are directly taken from Flynn and Hipkin (1999).

The Supplement related to this article is available online at https://doi.org/10.5194/bg-15-4333-2018-supplement.

Competing interests. The authors declare that they have no conflict of interest.

Special issue statement. This article is part of the special issue "Interactions between planktonic organisms and biogeochemical cycles across trophic and N_2 fixation gradients in the western tropical South Pacific Ocean: a multidisciplinary approach (OUTPACE experiment)". It is not associated with a conference.

Acknowledgements. We thank the ship captains, the scientists, and funding agencies of all the projects (OUTPACE, BIOSOPE, MOORSPICE, DIAPALIS, NECTALIS, PANDORA, Mirai) that allowed data collection without which we could not validate our model. The authors thank the Institute of Research for Development for supporting all authors. Cyril Dutheil is funded by European project INTEGRE.

Edited by: Thierry Moutin
Reviewed by: Andreas Oschlies and one anonymous referee

References

Arrigo, K. R.: Marine microorganisms and global nutrient cycles, Nature, 437, 349–355, https://doi.org/10.1038/nature04159, 2005.

Assmann, K. M., Bentsen, M., Segschneider, J., and Heinze, C.: An isopycnic ocean carbon cycle model, Geosci. Model Dev., 3, 143–167, https://doi.org/10.5194/gmd-3-143-2010, 2010.

Aumont, O. and Bopp, L.: Globalizing results from ocean in situ iron fertilization studies: GLOBALIZING IRON FERTILIZATION, Global Biogeochem. Cy., 20, GB2017, https://doi.org/10.1029/2005GB002591, 2006.

Aumont, O., Ethé, C., Tagliabue, A., Bopp, L., and Gehlen, M.: PISCES-v2: an ocean biogeochemical model for carbon and ecosystem studies, Geosci. Model Dev., 8, 2465–2513, https://doi.org/10.5194/gmd-8-2465-2015, 2015.

Bennett, S. A., Achterberg, E. P., Connelly, D. P., Statham, P. J., Fones, G. R., and German, C. R.: The distribution and stabilisation of dissolved Fe in deep-sea hydrothermal plumes, Earth Planet. Sc. Lett., 270, 157–167, https://doi.org/10.1016/j.epsl.2008.01.048, 2008.

Bergman, B., Sandh, G., Lin, S., Larsson, J., and Carpenter, E. J.: *Trichodesmium* – a widespread marine cyanobacterium with unusual nitrogen fixation properties, FEMS Microbiol. Rev., 37, 286–302, https://doi.org/10.1111/j.1574-6976.2012.00352.x, 2013.

Berman-Frank, I.: Segregation of Nitrogen Fixation and Oxygenic Photosynthesis in the Marine Cyanobacterium Trichodesmium, Science, 294, 1534–1537, https://doi.org/10.1126/science.1064082, 2001.

Berthelot, H., Bonnet, S., Camps, M., Grosso, O., and Moutin, T.: Assessment of the dinitrogen released as ammonium and dissolved organic nitrogen by unicellular and filamentous marine diazotrophic cyanobacteria grown in culture, Frontiers in Marine Science, 2, 80, https://doi.org/10.3389/fmars.2015.00080, 2015a.

Berthelot, H., Moutin, T., L'Helguen, S., Leblanc, K., Hélias, S., Grosso, O., Leblond, N., Charrière, B., and Bonnet, S.: Dinitrogen fixation and dissolved organic nitrogen fueled primary production and particulate export during the VAHINE mesocosm experiment (New Caledonia lagoon), Biogeosciences, 12, 4099–4112, https://doi.org/10.5194/bg-12-4099-2015, 2015b.

Berthelot, H., Bonnet, S., Grosso, O., Cornet, V., and Barani, A.: Transfer of diazotroph-derived nitrogen towards non-diazotrophic planktonic communities: a comparative study between Trichodesmium erythraeum, Crocosphaera watsonii and *Cyanothece* sp., Biogeosciences, 13, 4005–4021, https://doi.org/10.5194/bg-13-4005-2016, 2016.

Berthelot, H., Benavides, M., Moisander, P. H., Grosso, O., and Bonnet, S.: High-nitrogen fixation rates in the particulate and dissolved pools in the Western Tropical Pacific (Solomon and Bismarck Seas): N_2 Fixation in the Western Pacific, Geophys. Res. Lett., 44, 8414–8423, https://doi.org/10.1002/2017GL073856, 2017.

Bissett, W., Walsh, J., Dieterle, D., and Carder, K.: Carbon cycling in the upper waters of the Sargasso Sea: I. Numerical simulation of differential carbon and nitrogen fluxes, Deep-Sea Res. Pt. I, 46, 205–269, https://doi.org/10.1016/S0967-0637(98)00062-4, 1999.

Bombar, D., Paerl, R. W., and Riemann, L.: Marine Non-Cyanobacterial Diazotrophs: Moving beyond Molecular Detection, Trends Microbiol., 24, 916–927, https://doi.org/10.1016/j.tim.2016.07.002, 2016.

Bonnet, S., Biegala, I. C., Dutrieux, P., Slemons, L. O., and Capone, D. G.: Nitrogen fixation in the western equatorial Pacific: Rates, diazotrophic cyanobacterial size class distribution, and biogeochemical significance: N_2 fixation in the equatorial pacific, Global Biogeochem. Cy., 23, GB3012, https://doi.org/10.1029/2008GB003439, 2009.

Bonnet, S., Rodier, M., Turk-Kubo, K. A., Germineaud, C., Menkes, C., Ganachaud, A., Cravatte, S., Raimbault, P., Campbell, E., Quéroué, F., Sarthou, G., Desnues, A., Maes, C., and Eldin, G.: Contrasted geographical distribution of N_2 fixation rates and *nif* H phylotypes in the Coral and Solomon Seas (southwestern Pacific) during austral winter conditions: N_2 fixation and diversity in the pacific, Global Biogeochem. Cy., 29, 1874–1892, https://doi.org/10.1002/2015GB005117, 2015.

Bonnet, S., Berthelot, H., Turk-Kubo, K., Cornet-Barthaux, V., Fawcett, S., Berman-Frank, I., Barani, A., Grégori, G., Dekaezemacker, J., Benavides, M., and Capone, D. G.: Diazotroph derived nitrogen supports diatom growth in the South West Pacific: A quantitative study using nanoSIMS: Transfer of diazotrophic N into plankton, Limnol. Oceanogr., 61, 1549–1562, https://doi.org/10.1002/lno.10300, 2016a.

Bonnet, S., Berthelot, H., Turk-Kubo, K., Fawcett, S., Rahav, E., L'Helguen, S., and Berman-Frank, I.: Dynamics of N_2 fixation and fate of diazotroph-derived nitrogen in a low-nutrient, low-chlorophyll ecosystem: results from the VAHINE mesocosm

experiment (New Caledonia), Biogeosciences, 13, 2653–2673, https://doi.org/10.5194/bg-13-2653-2016, 2016b.

Bonnet, S., Caffin, M., Berthelot, H., and Moutin, T.: Hot spot of N_2 fixation in the western tropical South Pacific pleads for a spatial decoupling between N_2 fixation and denitrification, P. Natl. Acad. Sci. USA, 114, E2800–E2801, 2017.

Bonnet, S., Caffin, M., Berthelot, H., Grosso, O., Benavides, M., Helias-Nunige, S., Guieu, C., Stenegren, M., and Foster, R. A.: In-depth characterization of diazotroph activity across the western tropical South Pacific hotspot of N_2 fixation (OUTPACE cruise), Biogeosciences, 15, 4215–4232, https://doi.org/10.5194/bg-15-4215-2018, 2018.

Breitbarth, E., Oschlies, A., and LaRoche, J.: Physiological constraints on the global distribution of *Trichodesmium* – effect of temperature on diazotrophy, Biogeosciences, 4, 53–61, https://doi.org/10.5194/bg-4-53-2007, 2007.

Breitbarth, E., Wohlers, J., Kläs, J., LaRoche, J., and Peeken, I.: Nitrogen fixation and growth rates of Trichodesmium IMS-101 as a function of light intensity, Mar. Ecol.-Prog. Ser., 359, 25–36, https://doi.org/10.3354/meps07241, 2008.

Böttjer, D., Dore, J. E., Karl, D. M., Letelier, R. M., Mahaffey, C., Wilson, S. T., Zehr, J., and Church, M. J.: Temporal variability of nitrogen fixation and particulate nitrogen export at Station ALOHA: Temporal variability of nitrogen fixation and particulate nitrogen, Limnol. Oceanogr., 62, 200–216, https://doi.org/10.1002/lno.10386, 2017.

Caffin, M., Moutin, T., Foster, R. A., Bouruet-Aubertot, P., Doglioli, A. M., Berthelot, H., Guieu, C., Grosso, O., Helias-Nunige, S., Leblond, N., Gimenez, A., Petrenko, A. A., de Verneil, A., and Bonnet, S.: N_2 fixation as a dominant new N source in the western tropical South Pacific Ocean (OUTPACE cruise), Biogeosciences, 15, 2565–2585, https://doi.org/10.5194/bg-15-2565-2018, 2018.

Capone, D. G.: Trichodesmium, a Globally Significant Marine Cyanobacterium, Science, 276, 1221–1229, https://doi.org/10.1126/science.276.5316.1221, 1997.

Carpenter, E. J.: Nitrogen Fixation by a Blue-Green Epiphyte on Pelagic Sargassum, Science, 178, 1207–1209, https://doi.org/10.1126/science.178.4066.1207, 1972.

Church, M. J., Jenkins, B. D., Karl, D. M., and Zehr, J. P.: Vertical distributions of nitrogen-fixing phylotypes at Stn ALOHA in the oligotrophic North Pacific Ocean, Aquat. Microb. Ecol., 38, 3–14, 2005.

Codispoti, L. A., Brandes, J. A., Christensen, J. P., Devol, A. H., Naqvi, S. A., Paerl, H. W., and Yoshinari, T.: The oceanic fixed nitrogen and nitrous oxide budgets: Moving targets as we enter the anthropocene?, Sci. Mar., 65, 85–105, https://doi.org/10.3989/scimar.2001.65s285, 2001.

Couvelard, X., Marchesiello, P., Gourdeau, L., and Lefèvre, J.: Barotropic Zonal Jets Induced by Islands in the Southwest Pacific, J. Phys. Oceanogr., 38, 2185–2204, https://doi.org/10.1175/2008JPO3903.1, 2008.

Cravatte, S., Madec, G., Izumo, T., Menkes, C., and Bozec, A.: Progress in the 3-D circulation of the eastern equatorial Pacific in a climate ocean model, Ocean Model., 17, 28–48, https://doi.org/10.1016/j.ocemod.2006.11.003, 2007.

Daines, S. J., Clark, J. R., and Lenton, T. M.: Multiple environmental controls on phytoplankton growth strategies determine adaptive responses of the N : P ratio, Ecol. Lett., 17, 414–425, https://doi.org/10.1111/ele.12239, 2014.

Da Silva, A. M., Young, C., and Levitus, S.: Algorithms and Procedures, in: Atlas of Surface Marine Data, Vol. 1, p. 83, NOAA Atlas Nesdis Edn., US Department of Commerce, National Oceanographic Data Center, User Services Branch, Washington, D.C., 1994.

Delmont, T. O., Quince, C., Shaiber, A., Esen, O. C., Lee, S. T. M., Lucker, S., and Eren, A. M.: Nitrogen-fixing populations of Planctomycetes and Proteobacteria are abundant in surface ocean metagenomes, Nat. Microbiol., 3, 804–813, https://doi.org/10.1038/s41564-018-0176-9, 2018.

Deutsch, C., Gruber, N., Key, R. M., Sarmiento, J. L., and Ganachaud, A.: Denitrification and N_2 fixation in the Pacific Ocean, Global Biogeochem. Cy., 15, 483–506, https://doi.org/10.1029/2000GB001291, 2001.

Deutsch, C., Sarmiento, J. L., Sigman, D. M., Gruber, N., and Dunne, J. P.: Spatial coupling of nitrogen inputs and losses in the ocean, Nature, 445, 163–167, https://doi.org/10.1038/nature05392, 2007.

Dunne, J. P., John, J. G., Shevliakova, E., Stouffer, R. J., Krasting, J. P., Malyshev, S. L., Milly, P. C. D., Sentman, L. T., Adcroft, A. J., Cooke, W., Dunne, K. A., Griffies, S. M., Hallberg, R. W., Harrison, M. J., Levy, H., Wittenberg, A. T., Phillips, P. J., and Zadeh, N.: GFDL–ESM2 Global Coupled Climate–Carbon Earth System Models. Part II: Carbon System Formulation and Baseline Simulation Characteristics, J. Climate, 26, 2247–2267, https://doi.org/10.1175/JCLI-D-12-00150.1, 2013.

Dupouy, C., Neveux, J., Subramaniam, A., Mulholland, M. R., Montoya, J. P., Campbell, L., Carpenter, E. J., and Capone, D. G.: Satellite captures trichodesmium blooms in the southwestern tropical Pacific, Eos T. Am. Geophys. Un., 81, 13–16, https://doi.org/10.1029/00EO00008, 2000.

Dupouy, C., Benielli-Gary, D., Neveux, J., Dandonneau, Y., and Westberry, T. K.: An algorithm for detecting *Trichodesmium* surface blooms in the South Western Tropical Pacific, Biogeosciences, 8, 3631–3647, https://doi.org/10.5194/bg-8-3631-2011, 2011.

Dutkiewicz, S., Ward, B. A., Monteiro, F., and Follows, M. J.: Interconnection of nitrogen fixers and iron in the Pacific Ocean: Theory and numerical simulations: marine nitrogen fixers and iron, Global Biogeochem. Cy., 26, GB1012, https://doi.org/10.1029/2011GB004039, 2012.

Falcón, L. I., Pluvinage, S., and Carpenter, E. J.: Growth kinetics of marine unicellular N-fixing cyanobacterial isolates in continuous culture in relation to phosphorus and temperature, Mar. Ecol.-Prog. Ser., 285, 3–9, 2005.

Fennel, K., Spitz, Y. H., Letelier, R. M., Abbott, M. R., and Karl, D. M.: A deterministic model for N_2 fixation at stn. ALOHA in the subtropical North Pacific Ocean, Deep-Sea Res. Pt. II, 49, 149–174, 2001.

Flynn, K. J. and Hipkin, C. R.: INTERACTIONS BETWEEN IRON, LIGHT, AMMONIUM, AND NITRATE: INSIGHTS FROM THE CONSTRUCTION OF A DYNAMIC MODEL OF ALGAL PHYSIOLOGY, J. Phycol., 35, 1171–1190, https://doi.org/10.1046/j.1529-8817.1999.3561171.x, 1999.

Flynn, K. J., Fasham, M. J., and Hipkin, C. R.: Modelling the interactions between ammonium and nitrate uptake in marine phytoplankton, Philos. T. Roy. Soc. B, 352, 1625–1645, 1997.

Gallon, J. R.: Reconciling the incompatible: N_2 fixation And O_2, New Phytol., 122, 571–609, https://doi.org/10.1111/j.1469-8137.1992.tb00087.x, 1992.

Galloway, J. N., Dentener, F. J., Capone, D. G., Boyer, E. W., Howarth, R. W., Seitzinger, S. P., Asner, G. P., Cleveland, C. C., Green, P. A., Holland, E. A., Karl, D. M., Michaels, A. F., Porter, J. H., Townsend, A. R., and Vörösmarty, C. J.: Nitrogen Cycles: Past, Present, and Future, Biogeochemistry, 70, 153–226, https://doi.org/10.1007/s10533-004-0370-0, 2004.

Garcia, N., Raimbault, P., and Sandroni, V.: Seasonal nitrogen fixation and primary production in the Southwest Pacific: nanoplankton diazotrophy and transfer of nitrogen to picoplankton organisms, Mar. Ecol.-Prog. Ser., 343, 25–33, https://doi.org/10.3354/meps06882, 2007.

Goebel, N. L., Edwards, C. A., Carter, B. J., Achilles, K. M., and Zehr, J. P.: Growth and carbon content of three different-sized diazotrophic cyanobacteria observed in the subtropical north pacific, J. Phycol., 44, 1212–1220, https://doi.org/10.1111/j.1529-8817.2008.00581.x, 2008.

Großkopf, T., Mohr, W., Baustian, T., Schunck, H., Gill, D., Kuypers, M. M. M., Lavik, G., Schmitz, R. A., Wallace, D. W. R., and LaRoche, J.: Doubling of marine dinitrogen-fixation rates based on direct measurements, Nature, 488, 361–364, https://doi.org/10.1038/nature11338, 2012.

Gruber, N.: Oceanography: A bigger nitrogen fix, Nature, 436, 786–787, 2005.

Gruber, N.: The Marine Nitrogen Cycle: Overview and challenges, in: Nitrogen in the Marine Environment, 1–50, Elsevier, https://doi.org/10.1016/B978-0-12-372522-6.00001-3, 2008.

Guieu, C., Bonnet, S., Petrenko, A., Menkes, C., Chavagnac, V., Desboeufs, K., Maes, C., and Moutin, T.: Iron from a submarine source impacts the productive layer of the Western Tropical South Pacific (WTSP), Sci. Rep.-UK, 8, 9075, https://doi.org/10.1038/s41598-018-27407-z, 2018.

Halm, H., Lam, P., Ferdelman, T. G., Lavik, G., Dittmar, T., LaRoche, J., D'Hondt, S., and Kuypers, M. M.: Heterotrophic organisms dominate nitrogen fixation in the South Pacific Gyre, ISME J., 6, 1238–1249, https://doi.org/10.1038/ismej.2011.182, 2012.

Hawser, S. P., O'Neil, J. M., Roman, M. R., and Codd, G. A.: Toxicity of blooms of the cyanobacterium Trichodesmium to zooplankton, J. Appl. Phycol., 4, 79–86, 1992.

Hood, R. R., Bates, N. R., Capone, D. G., and Olson, D. B.: Modeling the effect of nitrogen fixation on carbon and nitrogen fluxes at BATS, Deep-Sea Res. Pt. II, 48, 1609–1648, https://doi.org/10.1016/S0967-0645(00)00160-0, 2001.

Johnson, K. S., Chavez, F. P., and Friederich, G. E.: Continental-shelf sediment as a primary source of iron for coastal phytoplankton, Nature, 398, 697–700, https://doi.org/10.1038/19511, 1999.

Jullien, S., Menkes, C. E., Marchesiello, P., Jourdain, N. C., Lengaigne, M., Koch-Larrouy, A., Lefèvre, J., Vincent, E. M., and Faure, V.: Impact of Tropical Cyclones on the Heat Budget of the South Pacific Ocean, J. Phys. Oceanogr., 42, 1882–1906, https://doi.org/10.1175/JPO-D-11-0133.1, 2012.

Jullien, S., Marchesiello, P., Menkes, C. E., Lefèvre, J., Jourdain, N. C., Samson, G., and Lengaigne, M.: Ocean feedback to tropical cyclones: climatology and processes, Clim. Dynam., 43, 2831–2854, https://doi.org/10.1007/s00382-014-2096-6, 2014.

Karl, D., Letelier, R., Tupas, L., Dore, J., Christian, J., and Hebel, D.: The role of nitrogen fixation in biogeochemical cycling in the subtropical North Pacific Ocean, Nature, 388, 533–538, 1997.

Kessler, W. S. and Gourdeau, L.: The Annual Cycle of Circulation of the Southwest Subtropical Pacific, Analyzed in an Ocean GCM*, J. Phys. Oceanogr., 37, 1610–1627, https://doi.org/10.1175/JPO3046.1, 2007.

Klausmeier, C. A., Litchman, E., Daufresne, T., and Levin, S. A.: Optimal nitrogen-to-phosphorus stoichiometry of phytoplankton, Nature, 429, 171–174, https://doi.org/10.1038/nature02454, 2004.

Krishnamurthy, A., Moore, J. K., Mahowald, N., Luo, C., Doney, S. C., Lindsay, K., and Zender, C. S.: Impacts of increasing anthropogenic soluble iron and nitrogen deposition on ocean biogeochemistry: atmospheric Fe and N and ocean biogoechemistry, Global Biogeochem. Cy., 23, GB3016, https://doi.org/10.1029/2008GB003440, 2009.

Kromkamp, J. and Walsby, A. E.: Buoyancy Regulation and Vertical Migration of Trichodesmium: a Computer-Model Prediction, in: Marine Pelagic Cyanobacteria: Trichodesmium and other Diazotrophs, edited by: Carpenter, E. J., Capone, D. G., and Rueter, J. G., 239–248, Springer Netherlands, Dordrecht, https://doi.org/10.1007/978-94-015-7977-3_15, 1992.

Kustka, A. B., Sanudo-Wilhelmy, S. A., Carpenter, E. J., Capone, D., Burns, J., and Sunda, W. G.: Iron requirements for dinitrogen- and ammonium-supported growth in cultures of Trichodesmium (IMS 101): Comparison with nitrogen fixation rates and iron: carbon ratios of field populations, Limnol. Oceanogr., 48, 1869–1884, 2003.

Kwiatkowski, L., Aumont, O., Bopp, L., and Ciais, P.: The Impact of Variable Phytoplankton Stoichiometry on Projections of Primary Production, Food Quality, and Carbon Uptake in the Global Ocean, Global Biogeochem. Cy., 32, 516–528, https://doi.org/10.1002/2017GB005799, 2018.

Küpper, H., etlk, I., Seibert, S., Pril, O., Etlikova, E., Strittmatter, M., Levitan, O., Lohscheider, J., Adamska, I., and Berman-Frank, I.: Iron limitation in the marine cyanobacterium *Trichodesmium* reveals new insights into regulation of photosynthesis and nitrogen fixation, New Phytol., 179, 784–798, https://doi.org/10.1111/j.1469-8137.2008.02497.x, 2008.

Large, W. G., McWilliams, J. C., and Doney, S. C.: Oceanic vertical mixing: A review and a model with a nonlocal boundary layer parameterization, Rev. Geophys., 32, 363, https://doi.org/10.1029/94RG01872, 1994.

LaRoche, J. and Breitbarth, E.: Importance of the diazotrophs as a source of new nitrogen in the ocean, J. Sea Res., 53, 67–91, https://doi.org/10.1016/j.seares.2004.05.005, 2005.

Letelier, R. and Karl, D.: *Trichodesmium* spp. physiology and nutrient fluxes in the North Pacific subtropical gyre, Aquat. Microb. Ecol., 15, 265–276, https://doi.org/10.3354/ame015265, 1998.

Luo, Y.-W., Doney, S. C., Anderson, L. A., Benavides, M., Berman-Frank, I., Bode, A., Bonnet, S., Boström, K. H., Böttjer, D., Capone, D. G., Carpenter, E. J., Chen, Y. L., Church, M. J., Dore, J. E., Falcón, L. I., Fernández, A., Foster, R. A., Furuya, K., Gómez, F., Gundersen, K., Hynes, A. M., Karl, D. M., Kitajima, S., Langlois, R. J., LaRoche, J., Letelier, R. M., Marañón, E., McGillicuddy Jr., D. J., Moisander, P. H., Moore, C. M., Mouriño-Carballido, B., Mulholland, M. R., Needoba, J. A., Orcutt, K. M., Poulton, A. J., Rahav, E., Raimbault, P., Rees,

A. P., Riemann, L., Shiozaki, T., Subramaniam, A., Tyrrell, T., Turk-Kubo, K. A., Varela, M., Villareal, T. A., Webb, E. A., White, A. E., Wu, J., and Zehr, J. P.: Database of diazotrophs in global ocean: abundance, biomass and nitrogen fixation rates, Earth Syst. Sci. Data, 4, 47–73, https://doi.org/10.5194/essd-4-47-2012, 2012.

Luo, Y.-W., Lima, I. D., Karl, D. M., Deutsch, C. A., and Doney, S. C.: Data-based assessment of environmental controls on global marine nitrogen fixation, Biogeosciences, 11, 691–708, https://doi.org/10.5194/bg-11-691-2014, 2014.

Maier-Reimer, E., Kriest, I., Segschneider, J., and Wetzel, P.: The Hamburg Ocean Carbon Cycle Model HAMOCC5 – Technical Description Release 1.1, Reports on earth system science, 14, available at: http://eprints.uni-kiel.de/14321/1/erdsystem_14.pdf (last access: 12 July 2018), 2005.

Marchesiello, P., McWilliams, J. C., and Shchepetkin, A.: Open boundary conditions for long-term integration of regional oceanic models, Ocean Model., 3, 1–20, https://doi.org/10.1016/S1463-5003(00)00013-5, 2001.

Marchesiello, P., Lefèvre, J., Vega, A., Couvelard, X., and Menkes, C.: Coastal upwelling, circulation and heat balance around New Caledonia's barrier reef, Mar. Pollut. Bull., 61, 432–448, https://doi.org/10.1016/j.marpolbul.2010.06.043, 2010.

Meunier, C. L., Malzahn, A. M., and Boersma, M.: A New Approach to Homeostatic Regulation: Towards a Unified View of Physiological and Ecological Concepts, PLoS ONE, 9, e107737, https://doi.org/10.1371/journal.pone.0107737, 2014.

Mills, M. M., Ridame, C., Davey, M., La Roche, J., and Geider, R. J.: Iron and phosphorus co-limit nitrogen fixation in the eastern tropical North Atlantic, Nature, 429, 292–294, 2004.

Mohr, W., Großkopf, T., Wallace, D. W. R., and LaRoche, J.: Methodological Underestimation of Oceanic Nitrogen Fixation Rates, PLoS ONE, 5, e12583, https://doi.org/10.1371/journal.pone.0012583, 2010.

Moisander, P. H., Beinart, R. A., Voss, M., and Zehr, J. P.: Diversity and abundance of diazotrophic microorganisms in the South China Sea during intermonsoon, ISME J., 2, 954–967, 2008.

Moisander, P. H., Beinart, R. A., Hewson, I., White, A. E., Johnson, K. S., Carlson, C. A., Montoya, J. P., and Zehr, J. P.: Unicellular cyanobacterial distributions broaden the oceanic N_2 fixation domain, Science, 327, 1512–1514, 2010.

Moisander, P. H., Benavides, M., Bonnet, S., Berman-Frank, I., White, A. E., and Riemann, L.: Chasing after Non-cyanobacterial Nitrogen Fixation in Marine Pelagic Environments, Front. Microbiol., 8, 1736, https://doi.org/10.3389/fmicb.2017.01736, 2017.

Monteiro, F. M., Dutkiewicz, S., and Follows, M. J.: Biogeographical controls on the marine nitrogen fixers: controls on marine nitrogen fixers, Global Biogeochem. Cy., 25, GB2003, https://doi.org/10.1029/2010GB003902, 2011.

Montoya, J. P., Holl, C. M., Zehr, J. P., Hansen, A., Villareal, T. A., and Capone, D. G.: High rates of N_2 fixation by unicellular diazotrophs in the oligotrophic Pacific Ocean, Nature, 430, 1027–1032, https://doi.org/10.1038/nature02824, 2004.

Moore, C. M., Mills, M. M., Arrigo, K. R., Berman-Frank, I., Bopp, L., Boyd, P. W., Galbraith, E. D., Geider, R. J., Guieu, C., Jaccard, S. L., Jickells, T. D., La Roche, J., Lenton, T. M., Mahowald, N. M., Marañón, E., Marinov, I., Moore, J. K., Nakatsuka, T., Oschlies, A., Saito, M. A., Thingstad, T. F., Tsuda, A., and Ulloa, O.: Processes and patterns of oceanic nutrient limitation, Nat. Geosci., 6, 701–710, https://doi.org/10.1038/ngeo1765, 2013.

Moore, J. K., Doney, S. C., Kleypas, J. A., Glover, D. M., and Fung, I. Y.: An intermediate complexity marine ecosystem model for the global domain, Deep-Sea Res. Pt. II, 49, 403–462, 2001.

Moore, J. K., Doney, S. C., and Lindsay, K.: Upper ocean ecosystem dynamics and iron cycling in a global three-dimensional model: global ecosystem-biogeochemical model, Global Biogeochem. Cy., 18, GB4028, https://doi.org/10.1029/2004GB002220, 2004.

Moore, J. K., Doney, S. C., Lindsay, K., Mahowald, N., and Michaels, A. F.: Nitrogen fixation amplifies the ocean biogeochemical response to decadal timescale variations in mineral dust deposition, Tellus B, 58, 560–572, https://doi.org/10.1111/j.1600-0889.2006.00209.x, 2006.

Moutin, T., Van Den Broeck, N., Beker, B., Dupouy, C., Rimmelin, P., and Le Bouteiller, A.: Phosphate availability controls Trichodesmium spp. biomass in the SW Pacific Ocean, Mar. Ecol.-Prog. Ser., 297, 15–21, 2005.

Moutin, T., Karl, D. M., Duhamel, S., Rimmelin, P., Raimbault, P., Van Mooy, B. A. S., and Claustre, H.: Phosphate availability and the ultimate control of new nitrogen input by nitrogen fixation in the tropical Pacific Ocean, Biogeosciences, 5, 95–109, https://doi.org/10.5194/bg-5-95-2008, 2008.

Mulholland, M. R. and Capone, D. G.: The nitrogen physiology of the marine N_2-fixing cyanobacteria *Trichodesmium* spp., Trends Plant Sci., 5, 148–153, https://doi.org/10.1016/S1360-1385(00)01576-4, 2000.

Mulholland, M. R. and Capone, D. G.: Stoichiometry of nitrogen and carbon utilization in cultured populations of Trichodesmium IMS101: Implications for growth, Limnol. Oceanogr., 46, 436–443, 2001.

Mulholland, M. R., Ohki, K., and Capone, D. G.: Nutrient controls on nitrogen uptake and metabolism by natural populations and cultures of Trichodesmium (cyanobacteria), J. Phycol., 37, 1001–1009, https://doi.org/10.1046/j.1529-8817.2001.00080.x, 2001.

Neveux, J., Tenírio, M. M. B., Dupouy, C., and Villareal, T. A.: Spectral diversity of phycoerythrins and diazotroph abundance in tropical waters, Limnol. Oceanogr., 51, 1689–1698, https://doi.org/10.4319/lo.2006.51.4.1689, 2006.

Ohki, K., Zehr, J. P., and Fujita, Y.: Regulation of nitrogenase activity in relation to the light-dark regime in the filamentous nonheterocystous cyanobacterium *Trichodesmium* sp. NIBB 1067, Microbiology, 138, 2679–2685, 1992.

O'Neil, J. and Romane, M.: Grazers and Associated Organisms of Trichodesmium, in: Marine Pelagic Cyanobacteria: Trichodesmium and other Diazotrophs, Vol. 362, Springer Netherlands, Dordrecht, 1992.

Paerl, H. W., Priscu, J. C., and Brawner, D. L.: Immunochemical localization of nitrogenase in marine Trichodesmium aggregates: Relationship to N_2 fixation potential, Appl. Environ. Microbiol., 55, 2965–2975, 1989.

Pahlow, M. and Oschlies, A.: Chain model of phytoplankton P, N and light colimitation, Mar. Ecol.-Prog. Ser., 376, 69–83, https://doi.org/10.3354/meps07748, 2009.

Penven, P., Debreu, L., Marchesiello, P., and McWilliams, J. C.: Evaluation and application of the ROMS 1-way embedding procedure to the central california upwelling system, Ocean Model.,

12, 157–187, https://doi.org/10.1016/j.ocemod.2005.05.002, 2006.

Postgate, J. R.: Biology nitrogen fixation: fundamentals, Philos. T. Roy. Soc. B, 296, 375–385, 1982.

Radic, A., Lacan, F., and Murray, J. W.: Iron isotopes in the seawater of the equatorial Pacific Ocean: New constraints for the oceanic iron cycle, Earth Planet. Sc. Lett., 306, 1–10, https://doi.org/10.1016/j.epsl.2011.03.015, 2011.

Raimbault, P. and Garcia, N.: Evidence for efficient regenerated production and dinitrogen fixation in nitrogen-deficient waters of the South Pacific Ocean: impact on new and export production estimates, Biogeosciences, 5, 323–338, https://doi.org/10.5194/bg-5-323-2008, 2008.

Ramamurthy, V. D. and Krishnamurthy, S.: Effects of N : P ratios on the uptake of nitrate and phosphate by laboratory cultures of Trichodesmium erythraeum (Ehr.), Proceedings: Plant Sciences, 65, 43–48, 1967.

Raven, J. A.: The iron and molybdenum use efficiencies of plant growth with different energy, carbon and nitrogen sources, New Phytol., 109, 279–287, https://doi.org/10.1111/j.1469-8137.1988.tb04196.x, 1988.

Rubin, M., Berman-Frank, I., and Shaked, Y.: Dust- and mineral-iron utilization by the marine dinitrogen-fixer Trichodesmium, Nat. Geosci., 4, 529–534, https://doi.org/10.1038/ngeo1181, 2011.

Rueter, J. G.: Iron stimulation of photosynthesis and nitrogen fixation in Anabaena 7120 and Trichodesmium (Cyanophyceae), J. Phycol., 24, 249–254, https://doi.org/10.1111/j.1529-8817.1988.tb04240.x, 1988.

Shchepetkin, A. F. and McWilliams, J. C.: The regional oceanic modeling system (ROMS): a split-explicit, free-surface, topography-following-coordinate oceanic model, Ocean Model., 9, 347–404, https://doi.org/10.1016/j.ocemod.2004.08.002, 2005.

Shiozaki, T., Kodama, T., Kitajima, S., Sato, M., and Furuya, K.: Advective transport of diazotrophs and importance of their nitrogen fixation on new and primary production in the western Pacific warm pool, Limnol. Oceanogr., 58, 49–60, https://doi.org/10.4319/lo.2013.58.1.0049, 2013.

Shiozaki, T., Kodama, T., and Furuya, K.: Large-scale impact of the island mass effect through nitrogen fixation in the western South Pacific Ocean: island mass effect through N_2 fixation, Geophys. Res. Lett., 41, 2907–2913, https://doi.org/10.1002/2014GL059835, 2014.

Shiozaki, T., Nagata, T., Ijichi, M., and Furuya, K.: Nitrogen fixation and the diazotroph community in the temperate coastal region of the northwestern North Pacific, Biogeosciences, 12, 4751–4764, https://doi.org/10.5194/bg-12-4751-2015, 2015.

Staal, M., Meysman, F. J. R., and Stal, L. J.: Temperature excludes N_2-fixing heterocystous cyanobacteria in the tropical oceans, Nature, 425, 501–504, https://doi.org/10.1038/nature02001, 2003.

Stenegren, M., Caputo, A., Berg, C., Bonnet, S., and Foster, R. A.: Distribution and drivers of symbiotic and free-living diazotrophic cyanobacteria in the western tropical South Pacific, Biogeosciences, 15, 1559–1578, https://doi.org/10.5194/bg-15-1559-2018, 2018.

Sterner, R. W. and Elser, J. J.: Ecological Stoichiometry: The Biology of Elements from Molecules to the Biosphere, https://doi.org/10.1515/9781400885695, 2002.

Sunda, W. G. and Huntsman, S. A.: Interrelated influence of iron, light and cell size on marine phytoplankton growth, Nature, 390, 389–392, https://doi.org/10.1038/37093, 1997.

Tagliabue, A., Bopp, L., and Aumont, O.: Ocean biogeochemistry exhibits contrasting responses to a large scale reduction in dust deposition, Biogeosciences, 5, 11–24, https://doi.org/10.5194/bg-5-11-2008, 2008.

Tagliabue, A., Bopp, L., Dutay, J.-C., Bowie, A. R., Chever, F., Jean-Baptiste, P., Bucciarelli, E., Lannuzel, D., Remenyi, T., Sarthou, G., Aumont, O., Gehlen, M., and Jeandel, C.: Hydrothermal contribution to the oceanic dissolved iron inventory, Nat. Geosci., 3, 252–256, https://doi.org/10.1038/ngeo818, 2010.

Tagliabue, A., Mtshali, T., Aumont, O., Bowie, A. R., Klunder, M. B., Roychoudhury, A. N., and Swart, S.: A global compilation of dissolved iron measurements: focus on distributions and processes in the Southern Ocean, Biogeosciences, 9, 2333–2349, https://doi.org/10.5194/bg-9-2333-2012, 2012.

Tegen, I. and Fung, I.: Contribution to the atmospheric mineral aerosol load from land surface modification, J. Geophys. Res., 100, 18707, https://doi.org/10.1029/95JD02051, 1995.

Toner, B. M., Fakra, S. C., Manganini, S. J., Santelli, C. M., Marcus, M. A., Moffett, J. W., Rouxel, O., German, C. R., and Edwards, K. J.: Preservation of iron(II) by carbon-rich matrices in a hydrothermal plume, Nat. Geosci., 2, 197–201, https://doi.org/10.1038/ngeo433, 2009.

Turk-Kubo, K. A., Karamchandani, M., Capone, D. G., and Zehr, J. P.: The paradox of marine heterotrophic nitrogen fixation: abundances of heterotrophic diazotrophs do not account for nitrogen fixation rates in the Eastern Tropical South Pacific: N_2-fixing potential of heterotrophs in the ETSP, Environ. Microbiol., 16, 3095–3114, https://doi.org/10.1111/1462-2920.12346, 2014.

Villareal, T. and Carpenter, E.: Buoyancy Regulation and the Potential for Vertical Migration in the Oceanic Cyanobacterium Trichodesmium, Microb. Ecol., 45, 1–10, https://doi.org/10.1007/s00248-002-1012-5, 2003.

Villareal, T. A. and Carpenter, E. J.: Diel buoyancy regulation in the marine diazotrophic cyanobacterium Trichodesmium thiebautii, Limnol. Oceanogr., 35, 1832–1837, https://doi.org/10.4319/lo.1990.35.8.1832, 1990.

White, A., Spitz, Y., and Letelier, R.: Modeling carbohydrate ballasting by Trichodesmium spp., Mar. Ecol.-Prog. Ser., 323, 35–45, https://doi.org/10.3354/meps323035, 2006.

Ye, Y., Völker, C., Bracher, A., Taylor, B., and Wolf-Gladrow, D. A.: Environmental controls on N_2 fixation by Trichodesmium in the tropical eastern North Atlantic Ocean – A model-based study, Deep-Sea Res. Pt. I, 64, 104–117, https://doi.org/10.1016/j.dsr.2012.01.004, 2012.

Zahariev, K., Christian, J. R., and Denman, K. L.: Preindustrial, historical, and fertilization simulations using a global ocean carbon model with new parameterizations of iron limitation, calcification, and N_2 fixation, Prog. Oceanogr., 77, 56–82, https://doi.org/10.1016/j.pocean.2008.01.007, 2008.

Zehr, J. P. and Bombar, D.: Marine Nitrogen Fixation: Organisms, Significance, Enigmas, and Future Directions, in: Biological Nitrogen Fixation, edited by: de Bruijn, F. J., 855–872, John Wiley & Sons, Inc., Hoboken, NJ, USA, https://doi.org/10.1002/9781119053095.ch84, 2015.